1-3 Zayda Northeastern Sector

This area is located on the northern boundary of the Zayda granite body. From the results of the first phase survey, it was apparent that many vein-like type uranium mineralizations within the shear zones were distributed in this area.

In this phase, semi-detailed and detailed surveys were performed in tracking these shear zones to clarify the distribution and scale of uranium mineralizations to study uranium concentrations in the vein structures.

Semi-detailed survey carried out by using topographic map of 1:10,000 scale for tracking shear zones and clarifying distributions of uranium mineralizations in them.

In detailed survey for the area having comparatively many uranium mineralizations, geological survey (using measuring types, pocket compass and scintilometer) and trenching were carried out.

1-3-1 Geology (PL. I-11-1 and 2)

In this area, granites of the Basement complex are exposed widely throughout the area, and P-T Red Sandstone Formation of Permo-Triassic system, T_1 Mudstone Formation of Tertiary system, Q_1 Siltstone Formation of Q_2 Siltstone Formation and β_1 Q_2 Basalt Lava of Quaternary system are found.

Major faults or shear zones trending NNE-SSW and N-S have developed, such as Amaragh Fault, GP-Vein shear and shear zones around Paneau-1, Ansagmir Fault etc.

(1) Granites

Granites intruded in the Hercynian age of the Paleozoic era are classified into granite, porphyritic granite, aplitic granite, aplite dyke, and granite porphyry dyke.

The granite is grey medium and coarse-grained and composed of feldspars, quartz and biotite of 4 to 5 mm. It is distributed principally south

of the Moulouya River. In the eastern part of this area, it is exposed extensively in the northern of Tighbouba-n-Ouzour and around Tassaksout-n-Assif-n-Malvit and Tassaksout ou Mougar. In the western part it is exposed in small scale near Assaka-n-Bou Idarn, Tichout Amazirig and Al Jaba, northeast of Zayda.

In general, porphyritic granite containing phenocrysts of 2 to 3 cm orthoclase has the transitional relation with the granite mentioned above. It is distributed principally north of the Moulouya River in this area. In this eastern part, it is exposed widely around Paneau-1 to eastern Bou Tazart and Bou Dilit, but in a small scale in the vicinity of Immayn-n-Ait Rahhou. In the western part, it is distributed along the Moulouya River, west of Assaka-n-Tabhirt.

Aplitic granite is fine-grained pink, and consists mainly of quartz and orthoclase, and accompanied by muscovite and biotite. It shows, in places, rock facies like pegmatite, having large crystals (several centimeters in diameter) of orthoclase and quartz. In the first phase survey, aplitic granite is clarified to distribute in the shape of gently sloping sheet of about 10 m thickness (maximum 40 m) near the surface of Zayda granite body. It is situated in topographical heights sloping gently toward the north, and occupies the majority of exposed granite area. And there are many kind of form of distribution such as lenticular and branched sheet like shapes in the peripheral area of Paneau-1, and several other complicated, dike, stock and sheet like shapes in the vicinity of Tasskout ou Mougar. It generally indicates rather high radioactivity in comparison with other granites.

Many aplite dykes are distributed in this area with various directions. Though they closely resemble aplitic granite in lithological facies, the grains are finer. Small dykes less than 1 m width are generally abundant,

but those of 3 to 4 m width are observed near Bou Tazart, east of Paneau-1.

Granite porphyry dykes are observed in the shear zones developed in granite bodies. In some places, it have anomalous radioactivity contrast with other granites. It consists of about 1 to 2 mm quartz phenocrysts and the groundmass of chocolate colored fine grains. As main dykes, there are small intermittent dykes in the GP-vein shear zone about 2 km west of Paneau 1, Paneau-1 East vein shear zone and Ansagmir Fault zone. The largest is in the GP-vein shear zone, where it has maximum width of more than 4 m.

(2) P-T Red Sandstone Formation

P-T Red Sandstone Formation are divided into coarse grain facies, principally consisting of arkose sandstone, and fine grain facies, principally consisting of red siltstone. In this phase survey, these are separately expressed on the geological maps. This formation gently dips north (less than 5°), and unconformably covers the granites.
As a results of the survey, depressions on granites and palaeocurrent could be presumed in some places.

Coarse grain facies: The coarse grain facies is a substratum of P-T Red Sandstone Formation and chiefly consists of arkose sandstone, but contains thin beds of sandstone and reddish brown siltstone in someplaces. This coarse grain facies is distributed in peripheral regions of Assaka-n-Bou Idarn, Al Jába and Aghanbou, Paneau-1 and Agard Azougagh, and the area from Bou Tazart to Immayn-n-Ait Rahhou on the eastern border of this area. Arkose sandstone chiefly consists of 2 to 3 mm fragments of quartz, feldspar and granite, and shows yellowish white in colour but, rarely shows conglomeratic facies containing granite pebbles of about 1 cm size.
In this area, the strata are thin, generally being 2 to 3 m thick, but they are developed locally in depressions of the Basement about 10 m. These depressions are found in the neighberhood of Assaka-n-Bou Idarn,

in the mining quarry of Tizi Tazougaght and in Bou Tazart east of Paneau-1.

In the peripheral region of Assaka-n-Bou Idarn, palaeocurrents running nearly north are presumed to be present in the quarry of the Zayda mine and near the village, where arkose sandstone accumilated thickly burying these palaeochannels. And at the banks of the Moulouya River, cross bedings are observed in arkose sandstone, in which palaeocurrents are assumed to run north.

In the quarry of Tizi Tazougaght excavation, arkose sandtone is about 1 m thick in the south, and more than 10 m in the north. The basement surface slopes gently northward, but in the results of the survey outer of this quarry, thick arkose sandstone was not discovered and the direction of palaeocurrent could not definite, therefore, it is probable that this is the depression of small scale without outlet, rather than the palaeocurrent.

In Bou Tazart east of Paneau 1, a polaeocurrent running N 45° W is presumed and conglomerate containing granite pebbles of about 1 cm size and arkose sandstone were deposited in to thickness of 10 m and about 100 m in width. On the arkose sandstone cliff which ran from Bau Tazart to the southeastern, besides the above mentioned palaeocurrent smaller scale polaeocurrents (10 to 20 m in width, and a few meters in depth) are presumable.

In the results of radioactivity prospectings carried out at the same time as the geological survey, no anomalous radioactivity could be found in these palaeocurrent routes.

Fine grain facies: The stratum of this facies is the upper of P-T Red Sandstone Formation consisting chiefly of nonstratified reddish brown siltstone with some thin beds of fine grain sandstone in the lower portion. In this area it is distributed in the hill of Rabouba and hills of Al Jába, Aghanbau etc.. It is also found on a small scale in the western and in the

western and in the north of Assaka-n-Tabbirt and in Tinzart-Tazougaght. In these regions, most of it has been erroded out and remains only 10 to 20 m at the above mentioned hills.

(3) T_1 Mudstone Formation

In this area, only calcareous conglomerate of this formation is found. This conglomerate is gray, 1 to 2 m in thickness, and composed of 3 to 5 cm limestone pebbles and calcareous matrix. This formation also occurs, in small scale, in the western part of this area unconformablly covering P-T Red Sandstone Formation.

(4) Q_1 Silt Formation

In this area, this formation consists of yellow siltstone and calcareous conglomerate contains pebbles of basalt and limestone. It is distributed in the top of hills in Rabouba, Al Jaba, Aghanbou. In Rabouba, yellow siltstone with about 10 m thick and calcareous conglomerate about 20 m thick cover P-T Red Sandstone Formation. In the hills of Aghaubou, Al Jaba and others, there is calcareous conglomerate of 2 to 3 m thick. The results of surveys so far indicate no anomalous radioactivity in outcrops of this Formation, but there are boulder of calcareous conglomerate in the southern part of Paneau-1, which is presumed to belong to this formation in which anomalous radioactivity is found.

(5) Q_2 Silt Formation

This formation consists of gray siltstone, medium-grained sandstone and calcareous conglomerate which are weakly consolidated. It is found at Ichmit in the western end in this area, in the north of Assaka-n-Tabbirt, and in Tazougught at the eastern end, etc.. In Ichmit, a small distribution of weakly consolidated conglomerate of this formation (is observed) and is covered by BQ_2 basaltic lava lappili. Medium-grained sandstone, calcareous

conglomerate and gray siltstone are distributed in the northern area of Assaka-n-Tabhirt, and the calcareous conglomerate is chiefly found in Tinzart-Tazougught.

(6) βQ_2 Basalt Lava

There is a lava dome in Ichmit at the western end of this area. This is generally composed of black and porous lava lappili, but, partially, volcanic conglomerate which contains heterogeneous pabbles such as limestone, granite and others besides basalt lappili.

1-3-2 Geological Structure

Since granites are exposed extensivelly in this area, the major geological structures are characterized by faults and shear zones. These are divided roughly into NNE-SSW system, N-S system, NW-SE system and others according to their strikes, but most of them are NNE-SSW system and N-S system and those which belong to NW-SE system are derived veins of small scale.

Main faults are as follows:

(1) Amaragh Fault

This fault runs through Amaragh-Ikhf-Qughanbou and is plainly observable on Moulouya River Sdes, where shear zone of 10 m or so is developed and it strikes N 35°E, and dips vertical. It cuts P-T Red Sandstone Formation. The vertical displacement is about 10 m. The west side is uplifted (the east side subsided). This is the only fault in this area which caused transition in P-T Red Sandstone Formation.

(2) G P vein shear zone

G P vein shear zone accompanies G P vein and in it the intrusion of granite porphyry dyke, which has anomalous radioactivities in some points, is observed. It is traceable from Tawiyat, west of Paneau-1 to Tighbouba-n-Ouzour. It is developed to be limited in the granite, and is covered with

P-T Red Sandstone Formation. The strike is N 35°W and inclination is vertical in the neighborhood of Moulouya River, but on tracking southward the strike changes to N 30°E - S30°W ~ N20°E - S20°W. The average width of shear zone is 20 to 30 m, but it reaches 50 m at the point crossing Moulouya River.

(3) Shear zones around Paneau-1

There are developed shear zones in granite extending from Paneau-1 toward the east, some parts of which has anomalous radioactivity.

Paneau-1 West vein shear zone: This shear zone has N 35°E strike and vertical inclination. It is traceable about 3 km from the western periphery of Paneau-1 mining quarry toward the southwest. The width of the zone is 1 to 5 m and it is covered with P-T Red Sandstone Formation.

Paneau-1 vein shear zone: This shear zone has N30°E strike and vertical inclination, and could be tracked about 4 km from the eastern periphery of Paneau-1 mining ruins toward the southwest. It intersects with N-S shear zone around Paneau-1 and shows N-S strike in some place. The width of the zone is 5 to 10 m throughout its length, but the width is more than 20 m where the strike changes direction.

Paneau-1 East vein shear zone: This zone is traceable southward extending more than 3.5 km from Agard Azougagh which is located 1 km east of Paneau-1. The strike is N-S and the inclination is vertical. This zone continues into P-T Red Sandstone Formation, but its' further continuation toward the north is not clear to be covered by the surface soil. But in Agard Azougagh, there is no transition in P-T Red Sandstone Formation. The width of the shear zone is 10 to 20 m, and many derived faults of NNE-SSW system are observed around it.

(4) Ansagmir Pault

Ansagmir fault is shear zone, developed along the Assif Ansagmir

River, a branch of the Moulouya River. Its total length reaches 8 km, and it is traceable from Immayn-n-Ait Rahhou toward Tassaksout ou Mougar in this area. The strike is N 30° E, and inclination is vertical, and AÏt Rahhou vein which is a portion of this zone contains uranium mineralization. The shear zone of this fault is about 40 m width and covered by P-T Red Sandstone Formation.

1-3-3 Lead Ore Deposits and Uranium Mineralizations.

In this area, there are stratified lead ore deposits in arkose sandstone, the lowermost of P-T Sandstone Formation and Vein-like type uranium mineralizations in the shear zone in granite and arkose sandstone just above shear zone. Major lead ore deposits have been excavated already by Zayda Mine and ruins of the excavation lie scattered around Assaka-n-Bou Idarn and in Tizi Tazougaght, Paneau-1 and its' peripheries.

Prospection for uranium has previously been carried out using the trenching and other methods on G P Vein, Paneau-1 vein and others, but none of them has been subject to development as yet.

(1) Lead ore deposits (PL. I-11-1, 2, Table 1-5)

Lead ore deposits which have not been mined yet are Ikhl Ouganbau mineralization located 2 km west of Assaka-n-Tabbirt, and AÏt Rahhou lead mineralization in Immayn-n-Ait Rahhou located at the eastern end of this area. In mineral tests, galena and cerussite were detected as lead minerals in both mineralization zones.

Ikhf Ouganbau mineralization: Disseminated galena is found in the 2 to 3 m of arkose sandstone which covers granites. The dissemination zone of 20 to 60 cm thick is distributed in 400 m length, along the arkose sandstone cliff on the south bank of Moulouya River. According to the results of analysis of 5 samples taken from this cliff at an interval of 100 m, this mineralization is a low grade containing Pb: 0.28 %

to 2.10 % and Ba: 3.60 to 8.80 %.

Aït Rahhou lead mineralization: This is distributed around Immayn-n-Ait Rahhou. The disseminated gallena zone is observed in 2 to 3 m thick arkose sandstone, and it is presumed approximately 400 m width and 1 km length. The thickness of the mineralized zone changes from 0.2 to 1.7 m, showing 1.7 m thickness at a small depression in the granite and reducing at its periphery to about 20 cm. Result of analysis of samples taken at 6 points shows Pb; 0.86 to 11.50 %, Ba; 0.30 to 9.60 %. Average thickness is 0.55 m and average grade is Pb; 6.47 %, Ba; 4.85 %. Pb grade is higher at the depression of granite as 4.7 to 9.8 %. Exploration boring for this mineralization has already been performed by Zayda Mine.

(2) Vein-like uranium mineralization (PL. 1-11-1, 2)

Major veins acompanied with uranium mineralization are Dique vein, Assaka-n-Tabhirt Vein, G P vein, Paneau-1 west vein, Paneau-1 vein, Paneau-1 east vein, Aït Rahhou north vein and Ait Rahhou south vein. In this phase survey, detailed geological surveys in the area around those and detailed radioactivity surveys for above mentioned veins, except Assaka-n-Tabhirt vein were performed, and trenching were carried out for Dique vein, Paneau-1 west vein and paneau-1 vein.

Dique vein (PL. I-12, Table I-6): This vein is located in the east bank of Moulouya River at the western end of this area. This vein has a shear zone developed in granite and anomalous radioactivity is found chiefly in ferruginous quartz vein in which its scale is small.

In this phase surveys, detailed geological survey of an area 600 x 700 m around this vein and trenching of 3 points 5.5 m in total were carried out. In this area, aplitic granite and arkose sandstone of P-T Red Sandstone covering unconformablly granites are observed. Shear zone in aplitic granite is overlain by arkose sandstone. It trends N 20°E and

dips vertical to 80°SE, with 2 to 4 m width and 40 m length along the branch of Moulouya River. Three layers of chocolate-colored 20 to 50 cm wide ferruginous quartz vein exist in this shear zone and anomalous radioactivity is found in and near this ferruginous quartz vein. As the result of geological and radioactive survey at three trenches of 20 m interval, and along the ferruginous quartz vein, the northern half of 20 m of the 40 m outcrop indicated radioactivity readings from 600 to 4200 c/s. Particularly, Trench-1 at the north end of the outcrop indicates high readings of radioactivity. But in the results of analysis of samples collected from trenches, the highest U content is 0.034 % (width of collection 50 cm) and significant analytical values could not be obtained. On the northward, this shear zone covered by arkose sandstone reappears to the surface at the 150 m north aparted from Trench-1, where it becomes to small scale of about 20 cm width and anomalous radioactivity could not be detected. On the Southward, its further extention is hardly recognizable because it has been covered by arkose sandstone and excavation wastes of Zayda Mine.

Assaka-n-Tabhirt vein: This vein occurs in Assaka-n-Tabhirt, the north bank of Moulouya River. It is small scale ferruginous quartz veins in granite and consists of 2 zones. Both are small veins of 10 cm width extending about 400 m. There are small fissures around them. Since detailed surveys for this vein had been performed in first phase survey, its' continuation toward the south was studied in this phase. The continuation of this vein was confirmed but no anomalous radioactivity was found, in the south of Moulouya River, and the anomalous radioactivity of 13500 c/s in small vein on the north bank does not continue to the south of Moulouya River. In the shear zone (width about 2 m) parrallel lying in the east side to this small veins, a small weak anomalous radioactivity of 600 c/s (continuation is about 3 m) was found in Moulouya River south bank.

In mineralogical examination for sample collected from the portion of 13500 c/s radioactivity, uranirite, bequerelite and carnotite were detected as uranium minerals.

G P vein (PL.I-13, Table I-6): This vein is composed of granite porphyry dyke, which is located about 2 km east of Assaka-n-Tabhirt. For this vein, 8 trenches had been performed in the past, so, in this phase, detailed geological survey for 600 m x 800 m area around this vein were carried out in parallel with sketeh of trenches, and radioactivity survey.
The results indicate that the width of the shear zone including this vein is 5 to 50 m, the strike is N 35°E - S 35°W and the inclination is vertical. The width increases from the northeast end toward the Moulouya River (toward the southwest), and there exist in it 2 dykes of graphite porphyry which branch off among the trenches T5 and T6. Radioactivity anomalies were detected chiefly at trenched and accompanied minute fissures in granite porphyry and ferruginous quartz veinlets. Each one is small in scale and 2 to 3 m in continuity. The shear zone extends more than 3.5 km southwestward crossing Moulouya River, but there was no anomalous radioactivity observed in the south of Moulouya River except the point of 300 c/s radioactivity at the site 500 m south from Moulouya River.

Paneau-1 West vein (PL. 1-14, Table I-6): This vein is shear zone extending from the westside of Paneau-1 excavation quarry toward the southwest, in which 2 zones of anomalous radioactivity were detected. One was detected in this shear zone and in arkose sandstone bed which lies just above and covering this shear zone. The other is located about 150 m east of it and is found in weathered granite and in arkose sandstone.

In this phase, detailed geological survey for Paneau-1 peripheries including, Paneau-1 vein and Paneau-1 east vein, approximately 1.5 km x 1.5 km, was carried out. A detailed geological radioactivity survey and

sketch of trenches as for this vein and its sorrounding area with its' peripheries were performed.

Anomalous radioactivity detectable in shear zone and arkose sandstone bed just above it exists at 2 points in the south of Moulouya River and in the excavated Paneau-1 quarry north of Moulouya River.

On 2 points in the south of Moulouya River trenches were made in the past and radioactivity readings from 300 to 1000 c/s were observed at T25 and 400 to 3000 c/s at T26. These anomalous radioactivity were detected along ferruginous quartz vein in the shear zone, but each continuity is short as 2 to 3 m in length. The analysis result of the sample taken from 3000 c/s radioactivity shows U: 0.026 %, Th: 0.010 %. By EPMA mineral examination uranium mineral was determined uraninite.

Anomalous radioactivities in portions covered by arkose sandstone such as at the Paneau-1 quarry were detected in minute fissures of the arkosic sandstone just above the shear zone and in the veinlets of barite. In the quarry, granite is partially exposed in places due to scraping off of arkose sandstone, where anomalous radioactivity readings of 900 to 1200 c/s were observed in the shear zone.

In the arkose sandstone covered its' extension, anomalous radioactivity of maximum 3000 c/s was detected around barite veinlets and analysis result of it shows U: 0.005 %, Th: $<$ 0.010 %. In the further northeast extension of the shear zone, there is an weak anomaly of 350 c/s in medium grained sandstone at 40 m west on the extension line. This weak anomaly is small and chemical analysis result of sample showed U: 0.009 %.

As the anomaly had been found the first phase survey about 150 m east of the above mentioned spot, 3 trenches for which, 32 m in total, was carried out in this phase. No remarkable shear zone was observed in granite, only assembled joints of N45°E - S45°W direction.

Weathering of granite arround this has developed. Within the border of granite and arkose sandstone and in the horizontal joints of weathered granite, black powder material (presumably manganese oxide) is deposited. Anomalous radioactivity was detected in weathered granite and arkose sandstone around this border. The distribution of the anomaly showing 300 c/s and above is small in scale, about 3 x 15 m. The results of the analysis of samples from the trench were averaged U: 0.010% (max. 0.020%).

Paneau-1 vein (PL. I-14, Table I-6) : This vein is located east of Paneau-1 quarry, about 500 m east from Paneau-1 west vein. In the first phase survey anomalous radioactivity distributions were revealed, consequently, in this phase, 20 trenches, 75 m in total, and detailed geological and radioactivity survey for it were performed in addition to detailed geological survey for the peripheries. Two shear zones of the N30°E and N-S trend exist in this area. They intersect at the east end of Paneau-1 quarry and are covered with arkose sandstone. Anomalous radioactivity was detected in the shear zone of the N30°E - S30°W system and in the arkose sandstone just above it. Two major anomalous zones exist in the excavation ruins, near the intersection with N-S system, and at the southeast end.

The anomalous zone near the intersection with the N-S system shows 3500 c/s radioactivity in maximum, but generaly, shows low radioactivity of 300 c/s to 1200 c/s. As the result of the detailed geological and radioactivity survey, the distribution of anomalous readings was defined as 5 to 6 m x 200 m approx. and these anomalous readings are scattered throughout this area. At the anomalous zone on 9 trenches, sketching and collection of samples were carried out, radioactivity of 3500 c/s was measured at T11 where about 10 cm of black powder material is deposited in the border of the granite and arkose sandstone indicating high reading.

The results of chemical analysis for samples show U: 0.012 % (Max. 0.025 %) on average.

The anomalous zone in the southeast end of the quarry is separated into 2 portions 8 trenches (T14-T21) in one portion and 3 trenches (T22-T24) in the other was performed. The anomalous zone of T14-T21 includes maximum reading of 8,000 c/s (in Trench 19), and its area over 300 c/s continues about 80 m. But the area over 1000 c/s is small in scale 3 m x 4 m (T14) and 2 m x 10 m (T18-T20). The results of chemical analysis for samples showed U: 0.059 % on average, including U: 0.33 % in maximum of which sample was taken from T19. Most specimens showed analysis values of less than U: 0.02%.

The anomalous zone of T22-T24 shows radioactivity of 2150 c/s in maximum, but generally,between 300 and 1500 c/s. The area over 300 c/s is about 2 x 15 m. Analysis of samples showed U: 0.021 % on average (maximum 0.068 %).

Paneau-1 East vein (PL. I-14, Table I-6): This vein is shear zone located 700 m east of Paneau-1. Anomalous readings of radioactivity are scattered in the shear zone of N-S and NE-SW direction trends on the north of Moulouya River. In this phase, detailed geological survey for its peripheries, detailed geological radioactivity survey for this vein and its surroundings and 1 trench (T27) were carried out. Resulting of these works, anomalous radioactivity readings were detected in ferruginous quatz veins and joints within the shear zone and each anomarous reading is

small in scale (0.1 m x 2 to 5 m). Indicating radioactivity shows range from 350 to 1500 c/s. In the N-S trend shear zone, 5 anomalous points are scattered over the length of 700 m, and in the NE-SW trend shar zone, 1 anomalous point exists near the intersection with the N-S trend shear zone. Chemical analysis results of samples taken from 3 points of 1500 c/s showed U: 0.014 to 0.056 %, Th: < 0.010 % and by EPMA mineral examination, uraninite, carnotite and paragenesis of bequerelite and fervanite were detected as uranium minerals.

Aït Rahhou North Vein (PL. I-15, Tabe I-6): This vein is located in Immagn-n-Aït Rahhou, the east end of the surveyed area, and occupies a section of Ansagmir Fault as Aït Rahhou south vein. In this phase, there were carried out detailed geological survey in the area of 400 x about 900 m around this vein and a detailed geological radioactivity survey for this vein.

The results show that the width of the shear zone is about 40 m in Immayn-n-Aït Rahhou, and it includes several veins of ferruginous quartz and dykes of granite porphyry (width about 40 cm) which are accompanied with barite veinlets. In these veins, it was clarified that weak anomalous radioactivities indicating 300 to 600 c/s have continued for 3 to 5 m. The result of chemical analysis for the sample of granite porphyry which indicated 600 c/s showed U: 0.020 %, Th : 0.010 %.

Aït Rahhou South Vein (PL. I-15, Table I-6): This vein is located about 1.5 km southeast of Aït Rahhou north vein. No anomalous radioactivity was detected in Ansagmir Fault between this vein and Aït Rahhou north vein.

In this phase, detailed geological survey for the area of 500 x 800 m around this vein and detailed radioactivity survey for this vein were performed. The survey results were similar to those for Aït Rahhou north vein; there are ferruginous quartz veins, barite veinlets and small dykes

of granite porphyry in the shear zone of 40 m width and several anomalous radioactivities were detected in them. The detailed survey was performed in about 800 m length, and anomalies of radioactivity were ascertained in 7 points. These are weak anomalies and are of small scale, showing 300 to 1200 c/s radioactivity and continuing for 1 to 3 m. Among them, analysis result of the point of 800 c/s radioactivity showed U; 0.010 % and Th: 0.010%.

Other uranium mineralizations (PL. I-11-1, 2): Other than the above mentioned, there are 3 uranium mineralization in Zayda NE Sector. One is shear zone located in the north bank of Moulouya River and in its' southside branch about 1 km west of Assaka-n-Tabhirt. This zone strikes N30°E, and dips vertical and the width is about 3 m. Ferruginous quartz Veins of small scale and about 5 cm width indicated anomalous radioactivity of 700 c/s in the north bank of Moulouya River, and of 1000 c/s in the southside branch. Analysis results of collected samples were U: 0.059 %, Th: 0.010 % (700 c/s) and U: 0.046 %, Th: 0.012 % (1000 c/s) respectively. The other containing ferruginous quartz strikes N40°E, dips vertical, and 5 cm width. They occur in the north bank of Moulouya River about 500 m east of Assaka-n-Tabhirt and shear zone in small creek about 1 km east of Ichmit, and show spot-like weak anomalies which 1200 c/s and 300 c/s radioactivity respectively.

1-3-4 Conclusion

(1) Lead Ore Deposits

In the results of this phase survey, it was confirmed that there were exsisted Ikhf Ouganbou lead mineralization and Aït Rahhou lead mineralization, in this area, as lead ore deposits which had not been excavated yet. Ikhf Ougenbau lead mineralization is of low grade, Pb: 0.28 % - 2.10 %, Ba: 3.60 % - 8.80 %, and of 20 to 60 cm thick. As the thickness of arkosic

sandstone bed (the host rock of ore deposit) is only 2 to 3 m, the possibility of it's future development is considered poor.

Aït Rahhou lead mineralization has mineralized zone of 0.2 to 1.70 m thick (average 0.55 m) and of Pb: 0.86 to 11.50 % (average 6.47 %), Ba: 0.30 to 9.60 % (average 4.85 %) grade.

Regard to this mineralization, though the exploration by boring had already been performed by Zayda Mine, there would be the possibility that ore deposit of high grade, but small in scale, might yet be discovered thorough future exploration programme in detail.

(2) Vein-like type uranium mineralizations

Uranium mineralizations in this area are related closely to the shear zones developed in granite, and radioactivity anomalies are detected in ferruginous quartz veins and granite porphyry dykes in shear zones and in arkose sandstone just above the shear zones.

These mineralization have been observed in eight areas which are within Dique vein, Assaka-n-Tabhirt vein, G P vein, Paneau-1 West vein, Paneau-1 vein, Paneau-1 East vein, Aït Rahhou north vein and Aït Rahhou south vein. Even the largest of them that is in Paneau-1 vein the anomalous radioactivity zone is of 5 to 6 m width and of about 200 m horizontal length. On the other hand, the maximum radioactivity reading in Paneau-1 vein was 8000 c/s and the maximum value of chemical analysis, was U: 0.33 % (width 1 m). But as to other mineralizations, their scale is less than several tens of meters, and grades are generally low, such as U; less than 0.020 % or 0.030 %.

Therefore it could be concluded that further exploration programme should not be positively promoted.

In this area, however, erosion of P-T Red Sandstone Formation has occurred such that thin arkose sandstone remains in the peripheries of

Paneau 1, and while uranium would be supposed to have been dissolved away during that erosion, it's radioactivity anomalies are rather dense and show high values compared with other districts. This fact suggests the possibility that this area could be source of uranium supplied into sedimentary strata. It should be, especially, worth noticing that, according to Radon Etch survey carried out in this phase the high anomalous zones were detected in the northeast extension of the above uranium mineralizations such as Paneau-1 vein and others, where is estimated the existence of palaeo-valleys by gravity survey of this phase.

Chapter 2 Radon Etch Survey

2-1 Radon Etch Method

2-1-1 Principles of the Radon Etch Method

In exploration for uranium mineral deposits, the geochemical prospecting method has received increasing attention in recent years. This method detects radon gas contained in lake water, river water, subsurface water and underground gas. The method has been extensively used, from preliminary surveys to detailed surveys with other geochemical and geophysical prospecting methods.

Radon, element 86 in the Periodic Table, is the heaviest member of the chemically inert rare gas group. There are three isotopes of radon: ^{222}Rn, ^{220}Rn (thoron) and ^{219}Rn (actinon). These three isotopes are daughter elements produced in the decay series of ^{238}U, ^{232}Th and ^{235}U.

As these three daughter elements are gaseous, they are both transported and diffused towards the ground surface. Accordingly, the presence of high concentrations of radon at the ground surface is suggestible presence of underground radioactive elements such as uranium and thorium as sources producing the radon.

This method has attracted attention as a method of estimating underground uranium using the above mentioned characteristics. Because of the low abundance of ^{235}U (0.7% of natural uranium), ^{219}Rn in nature is neglected in performance of this method.

The decay series of ^{238}U and ^{232}Th are shown in Fig. I-2. Radon is the 6th element in the series of ^{238}U and the 5th element in the series of ^{232}Th. Both elements are alpha emitters during decay.

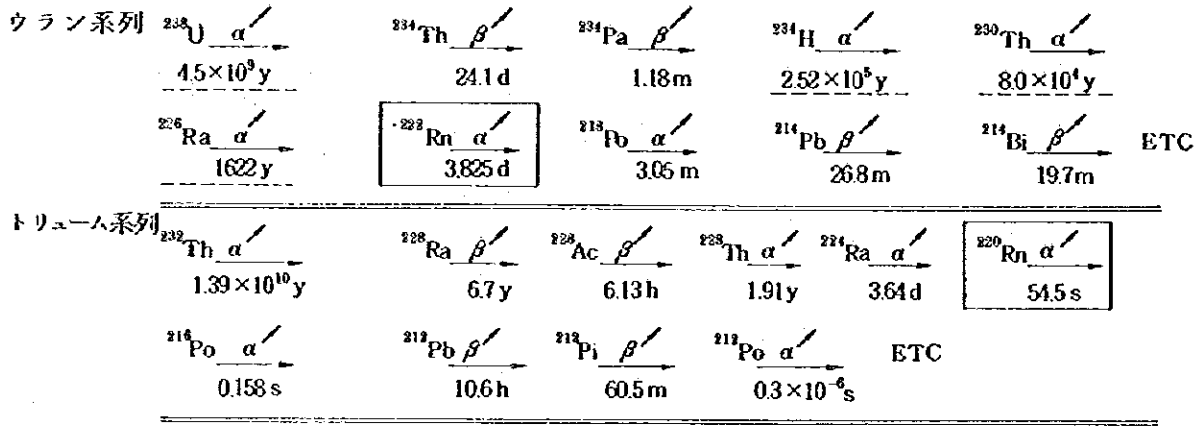

y = years
d = days
m = minutes
s = seconds
Elements above, ^{222}Rn of geochemical significance are underlined.

Fig. I—2 Partial Decay Series of ^{238}U and ^{232}Th

The principle of radon detection is based on the detection of alphas emitted during the decay of radon atoms and its daughters.

There are the following four principal ways of detecting alpha particles and several devices were developed and have been used.

- o Gold-leaf electroscope
- o Zinc sulphide sintillometer
- o Ionization chamber
- o Alpha-track method

Except the alpha-track method, the above methods detect alpha particles emitted from radon gas in samples from subsurface gas, river water, lake water, etc. However, these methods are not considered to be effective for prospecting uranium mineral deposit, because the equipment is complicated and the sampling time is short. In short sampling time, detected values deviate from each other; so, it is difficult to obtain

real values. It is assumable that the transport and diffusion of radon gas is influenced by atmospheric pressure, humidity, wind, water vapor and other weather conditions. Accordingly, it is generally considered that such phenomena greatly change the detected results.

In order to minimize these influences, it is necessary to lengthen the sampling time to eliminate the deviations of time and place. The alpha-track method was contrived recently to eliminate these problems, and it is extensively used in exploration for uranium mineral deposits.

The alpha-track method is based on the degradation of alpha particle energy. When alpha particles traverse solids, they undergo atomic collisions and leave evidence of their passage along each particle trajectory as a track. This method detects passage tracks and counts their number to determine the concentration of radon gas. To achieve this, an alpha-sensitive film has been manufactured. Cups attached this film are placed in detecting points and allowed to stand for specified period. After recovery, these cups are processed to facilitate observation, then the number of alpha particle passage tracks is counted. For analysis of the detecting results, the determination of the background range has much significance, as in the other geochemical prospecting, and will greatly affect the evaluation of survey results.

For the present survey, detector cups manufactured by Terradex, U.S.A. were purchased. Each cup had a cellulose nitrate film attached to the inner surface of its bottom. These cups were placed underground where they remained for 3 to 4 weeks. The recovered cups were returned to Terradex for processing and track-counting. The report on the analysis was duly received from Terradex.

In geochemical prospecting by detection of radon gas, the depth of detectable uranium mineral deposit is limited because of the length of

half-life of radon. Therefore, this method is not effective in the exploration for uranium mineral deposit to be in more than several hundred meters depth. From past experience, it is said that the maximum effective depth is about 200 m.

2-1-2 Application for Surveyed Area

The surveyed area is located in the north of Zayda and Bou Mia Granite Bodies. This area is the southern part of large basin structure between these granite bodies and the Moyen Atlas Mountains, as clarified in the previous surveys. Geologically, the basin consists mainly of P-T Red Sandstone Formation which is gradually dipping northwards. In both Zayda and Bou Mia granite areas, there are scattered arkose sandstone beds which are belonging to the lower part of P-T Red Sandstone Formation. All of the Palaeo-currents originated within the term of deposition of P-T Red Sandstone Formation, and which could be determined through ripple marks, sole marks and cross bedding in arkose sandstone, flow to the north. On both sides of the Moulouya River located near northern limit of the exposure area of Zayda Granite Body, shear zones, granite porphyry dikes and ferruginous-quartz veins which are in shear zone are extensively distributed. In these shear zones, dikes and veins, small scale radioactive anomalies were detected. According to the first phase survey, uranium mineralization has been found, in these shear zones or in the arkose sandstone of the lower part of P-T Red Sandstone Formation which are located immediately above shear zone. In addition to these other radioactive anomalies were detected in boulders, scattering near Paneau-1, of conglomerate belonging to Q_1 silt Formation and in the river sand of Moulouya River. Resulting these facts, in this region, uranium mineral deposits could be expected mostly in the shear zones which are developed in granite and its covertures, and in the lower part of P-T

Red Sandstone Formation. Through examples of the uranium mineral deposits in various parts of the world, it would be considerable that the possibility of uranium mineral deposits was large in the palaeo-currents originated in the term of deposition of P-T Red Sandstone Formation.

The present Radon Etch survey was carried out taking into consideration the geology, geological structure and features of uranium mineralization for the purpose of research the potential uranium mineral deposit in:

- o the north of the above-described shear zones, or
- o the palaeo-currents originated in the deposition of P-T Red Sandstone Formation, which could be expected to be in the southern part of the basin structure located in the north of Zayda-Bou Mia Granite Bodies.

For radon gas detection, the surveyed area was divided into three zones as described below, and the spacing between cups was decided for each zone.

(1) In the zone in which P-T Red Sandstone Formation is exposed or covered with thin Quaternary Formation, corresponding to the northern extension of the vein-like type uranium mineralization, the uranium mineral deposit would be expected to be in comparatively shallow depth, therefore, cups were placed at spacing of east-west 500 m and north-south 500 m.

(2) In the zones in which P-T Red Sandstone Formation is exposed but the presence of vein-like type uranium mineralization is not expected as the result of the first phase survey and also in which the presence of P-T Red Sandstone Formation is expected in rather deep in the ground because covered with Cretaceous system, etc., cups were placed at spacing of east-west 500 m and north-south 1,000 m.

(3) In the zone located outside the above zones and in which distribution of P-T Red Sandstone Formation could be expected to be in depth, cups were placed at spacing of east-west 1,000 m and north-south 1,000 m.

Before cups were placed, the thoron filter was installed in most of the cups to eliminate ^{220}Rn, the daughter element of ^{232}Th, because the objective was uranium exploration.

2-1-3 Operation

Radon gas detector cups were ordered in advance, received at Rabat Airport in Morocco, and transported to the surveyed area. For installation of cups in the north of Zayda Granite Body, a north-south base line was established near the fork of the road from Zayda to Sidi Ayyad and the road to Agoudim. The direction and spacing between cups were measured with measuring tapes and pocket-compasses. Then, cups were emplaced at the specified points. For the area from Itzar to the north of Bou Mia Granite Body, the cup installation points were decided by using the 1/25,000 scale topographic map enlarged from the 1/50,000 scale map. To locate cup placement points, direction and distance were measured with measuring tapes and pocket-compasses, on the basis of natural features indicated on the map. About 40 cm deep holes were dug with picks and shovels. Cups were placed in these holes after radioactivity at the bottom of each hole had been measured with SPP-2NF sintillometer. These cups were covered with vinyl sheet, then the holes were refilled with the displaced soil. The cups were allowed to remain for 20 to 26 days before being recovered. Recovered cups were returned to Terradex. Terradex completed processing, counted the number of tracks, conducted preliminary analysis, and prepared the report including the list of Radon Etch readings. The report was mailed to Tokyo after the survey team returning to Japan. After reviewing Terradex report, principal analysis with the computer was conducted for the

clarifying the relation between Radon Etch reading and geology on the cup installation places.

Several cups were not recovered because they were dug out from the ground, damaged or taken by residents of the area, shepherds, etc.

The operation is summarized as follows.

(1) Radon detector cups

Radon detector cups manufactured by Terradex (trade mark: Track-Etch Cups) were used. Each cup is plastic, about 7 cm in diameter and 10 cm long. Cellulose nitrate (CN) film, as the radon detector, is attached on the inner surface of cup bottom. Thoron filters were placed in each cup to eliminate ^{220}Rn.

(2) Number of placement points and cups

The number of placement points was 736. However, the total number of cups emplaced was 749 becuase some cups were emplaced to supplement damaged and improperly placed cups.

(3) Number of recovered cups

The total number of recovered cups was 679. Since the emplacement of 6 cups had not been satisfactory, data for them was not used in the analysis. Therefore, the number of effective recovered cups was 673.

(4) Cup placement period

Placement started on May 16, 1979 and ended on June 8, 1979.

(5) Cup recovery period

The recovery started on June 6, 1979 and ended on June 30, 1979.

(6) Period that cups were buried.

Minimum: 21 days

Maximum: 26 days

(7) Emplacement depth and holes

Forty centimeter deep holes were dug. Cups were placed so that the

cup opening faced the bottom of the hole. Each cup was covered with a vinyl sheet before being refilled with the displaced soil.

(8) Equipment and materials

For digging holes	:	shovels, picks and hammers
For measuring radioactivity	:	SPP-2NF sintillometer
For surveying	:	100 m long measuring tape and pocket-compass
Others	:	1/50,000 and 1/25,000 scale topographic maps, vinyl sheet, etc.

(9) Determination of cup placement positions

The positions were determined from the topography and natural features illustrated on the 1/25,000 scale topographic map. On flat land, the determination was made by using the base line, 1/25,000 scale topographic map, measuring tapes and pocket-compasses.

(10) Etch processing, track counting and preliminary analysis

The above were carried out by Terradex; the report and contour map being sent to the survey team.

(11) Time correction for differences in measurement periods (indication of measured values)

The number of tracks were calculated on the assumption that all cups were buried for 30 days. Measured values are expressed as T (tracks)/ sq.mm.30 days.

(12) Indication of cup placement position

Using the coordinates system of the 1/50,000 scale topographic map, the X axis (east-west), Y axis (north-south) and Z axis (meters above the sea level determined from the map) were indicate for each cup position.

(13) Principal analysis

Since geological conditions were not included in preliminary

analysis, the principal analysis on the survey results was conducted with computer to take into consideration the geology of the placement positions.

2-2 Survey Results

2-2-1 Table of Results

All data are tabulated in Table I-10, Radon Etch Survey Results. This table, excludes cups which could not be recovered (damaged or taken by residents). These data are indicated in the way discussed in the previous section.

The results were in range of 4.1 ~ 798.6 T/sq.mm.30 days. Cups damaged by residents or at the time of recovery are as follows.

Damaged	: 21
Film was cracked or contaminated.	: 6
Dug out by residents but returned to the hole and covered with soil	: 3
Dug out by residents and thoron filter removed.	: 2

Even though there were changes in cup conditions as described above, it can be said that such changes could not increase reading values because measured values were in the range from 17.3 to 161.5 T/sq.mm.30 days, which were within the background of Radon Etch readings to be discussed later.

Since the quantity of thoron filters was not sufficient, 8 filterless cups were placed in the western end of the surveyed area. Readings for these 8 filterless cups and cups which had the filter removed by residents were in range of 33.4 ~ 253.8 T/sq.mm.30 days. No remarkable difference was found between values for cups with the filter and those without.

2-2-2 Results of Data Analysis on the Basis of Frequency Distribution of Radon Etch Readings

The preliminary analysis by Terradex does not include geological

conditions. That is, data were processed assuming the same geological conditions for all readings. Therefore, the survey team conducted the principal analysis to take into consideration the geological conditions.

(1) Preliminary Analysis

The method of background determination used by Terradex is as follows.

- o Readings are ranked in order from the lowest to the highest.
- o The value for the mid-point of this sequence (M_1) is selected.
- o (M_1) is multiplied by 3.
- o Readings are placed in order from the lowest to 3X (M_1).
- o The value for the mid-point of this sequence (M_2) is selected.
- o M_2 is multiplied by 3. Readings are placed in order from the lowest to 3X (M_2), and the value at the mid-point of the sequence is obtained.
- o This procedure is repeated until (Mn) = (Mn-1).
- o When (Mn) = (Mn-1), (Mn) is multiplied by 3. This value of 3X (Mn) is taken as the upper limit of the background.
- o For the background determined by the above way, the normal statistical values, the mean value and standard deviation, are calculated.

The application of the above procedures to the present survey results is as follows. The total number of values is 679 which includes values for 6 cups placed improperly.

Procedure 1

1 ---------- 340 ---------- 679 ----------

4.1 T/sq.mm.30 days 80.1 T/sq.mm.30 days--798.0 T/sq.mm.30 days

80.1 T/sq.mm.30 days x 3 = 240.3 T/sq.mm.30 days

Procedure 2

1 ---------- 316 ---------- 632 ----------

4.1 T/sq.mm.30 days--74.2 T/sq.mm.30 days--238.1 T/sq.mm.30 days

74.2 T/sq.mm.30 days x 3 = 222.6 T/sq.mm.30 days

Procedure 3

1 ---------- 312 ---------- 624 ----------

4.1 T/sq.mm.30 days--73.3 T/sq.mm.30 days--219.8 T/sq.mm.30 days

73.3 T/sq.mm.30 days x 3 = 219.9 T/sq.mm.30 days

Procedure 4

1 ---------- 312 ---------- 624 ----------

4.1 T/sq.mm.30 days 73.3 T/sq.mm.30 days- 219.8 T/sq.mm.30 days

$M_4 = M_3 = 73.3$ T/sq.mm.30 days

Therefore, the upper limit of the background is:

73.3 T/sq.mm.30 days x 3 = 219.9 T/sq.mm.30 days

As the result of reviewing the frequency distribution around the upper limit of the background obtained by the above procedures, the upper limit of the background was found to be 216.3 T/sq.mm.30 days. In the analysis by Terradex, the 6 cups of which emplacement was not satisfactory were included for data analysis. The frequency distribution near the upper limit of the background in T/sq.mm.30 days was 2 at 201 ~ 202, 2 at 215.2, 1 at 216.3 and 2 at 219.8. From this distribution, it is possible to say that 216.3 T/sq.mm.30 days or less and 219.8 T/sq.mm.30 days or more form separate mother groups respectively. As result of the above calculation and reviewing the frequency distribution, Terradex gave 216.3 T/sq.mm.30 days as the upper limit of the background.

However, the above-mentioned 6 improperly placed cups should not be included in the data analysis. In reviewing the data for the 673 cups (excluding these 6 cups), the frequency distribution near the upper limit

of the background in T/sq.mm.30 days is 4 at 192.3, 1 at 194.7, 1 at 200.0, 1 at 201.9, and 2 at 215.2. Therefore, the boundary between the 2 mother groups is possibly between 201.9 T/sq.mm.30 days and 215.2 T/sq.mm.30 days. Based on the Terradex's concept of background, therefore, the upper limit of the background for reading values is 201.9 T/sq.mm.30 days. The background determined as above could be explained as follows. The distribution range of the background should be the low value range in which the most readings were included, and the frequency distribution could thus be concluded to be nearly normal. Results of this survey are discussed below.

Readings range from 4.1 to 798.0/sq.mm.30 days. Therefore, the range between 0 and 800 T/sq.mm.30 days is equally divided into 80. Histogram was prepared on the basis of readings in each 10 T/sq.mm.30 days section. This is shown in Fig. I-3, Statistical Diagram of Radon Etch Readings (in the preliminary analysis). This histogram shows a Poisson distribution (logarithmic normal distribution) if unevenness is neglected. However, since the number of readings was only 1 in 200 - 210 T/sq.mm.30 days, it could be considered that the mother group of readings divides into two for this range. The group 210 T/sq.mm.30 days or less represents low reading value region which has nearly normal distribution and includes most of the readings. Therefore, this region is considerable to be the mother group of the background. Splitting the sample group having Poisson distribution into two is not acceptable in the statistical standpoint. The Terradex use of this idea is perhaps based on their accumulated experience and data.

Statistical values of the mother group of the background are as follows.

Background mean (B.G.M.): 79.7 T/sq.mm.30 days

Standard deviation (σB) : 44.2 T/sq.mm.30 days

Classification of Radon Etch Readings (T/sq·mm·30days)	n : Number of Readings
0 — 10	5
10 — 20	23
20 — 30	54
30 — 40	47
40 — 50	56
50 — 60	59
60 — 70	52
70 — 80	40
80 — 90	55
90 — 100	38
100 — 110	42
110 — 120	31
120 — 130	24
130 — 140	23
140 — 150	18
150 — 160	16
160 — 170	10
170 — 180	10
180 — 190	9
190 — 200	6
200 — 210	1
210 — 220	5
220 — 230	4
230 — 240	4
240 — 250	5
250 — 260	3
260 — 270	2
270 — 280	4
280 — 290	2
290 — 300	2
300 — 310	
310 — 320	1
320 — 330	
330 — 340	2
340 — 350	
350 — 360	2
360 — 370	1
370 — 380	
380 — 390	
390 — 400	1
400 — 410	
410 — 420	
420 — 430	1
430 — 440	1
440 — 450	1
450 — 460	1
460 — 470	1
470 — 480	1
480 — 490	2
490 — 500	1
500 — 510	
510 — 520	
520 — 530	1
530 — 540	
540 — 550	
550 — 560	
560 — 570	
570 — 580	
580 — 590	
590 — 600	
600 — 610	
610 — 620	1
620 — 630	
630 — 640	
640 — 650	
650 — 660	
660 — 670	
670 — 680	1
680 — 690	1
690 — 700	
700 — 710	
710 — 720	
720 — 730	
730 — 740	
740 — 750	
750 — 760	1
760 — 770	
770 — 780	
780 — 790	
790 — 800	2
Total	673

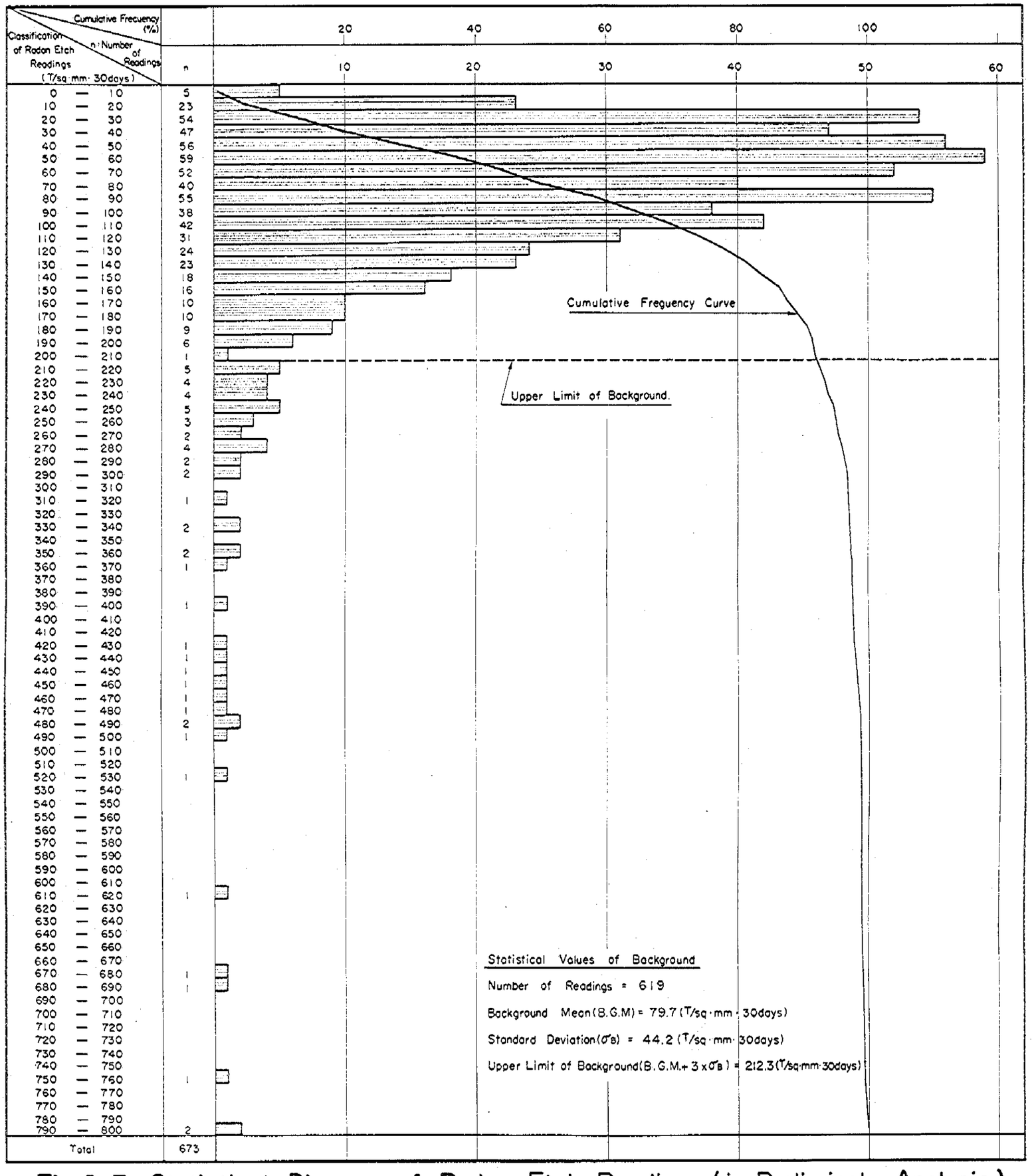

Fig. I-3 Statistical Diagram of Radon Etch Readings (in Preliminaly Analysis)

When the background range is determined as above, higher readings excluded from background must be considered to be anomalies. Terradex calculates Z value on the scale of standard variation for each reading value by using the background statistical values. The background ranges up to Z=3, for an anomaly Z>3. Ranking is indicated in multiples based on Z value and B.G.M. The Z value is determined by the following formula.

$Z = (x - B.G.M.)/\sigma B$ (x: reading value)

In this formula, the Z value shows the remoteness of reading value from B.G.M. If the distribution of the mother group of the background is taken as normal and its upper limit is (B.G.M. = 3 σB) containing about 99% of the mother group which has been estimated from the distribution of reading values, readings to Z = 3 must be judged as belonging to the background. If the upper limit of the background is (B.G.M. + 2 σB) which contains about 95% of the mother group, however, readings to Z = 2 must be judged as belonging to the background.

If (mean + 2 σ) would be the upper limit of the background - this was generally used for analysis of geochemical survey data, it could be said that readings for $2<Z<3$ are possible anomalous.

Terradex, therefore, took a background range as wide as possible considered Z = 3 as the upper limit of background. They further numerically clarified the background range determined by the above histogram, and determined that values exceeding 212.3 T/sq.mm.30 days = B.G.M. + 3 B = (79.7 + 3 x 44.2) T/sq.mm.30 days were anomalous.

The number of such anomalous values is 54 in total. The following are these values classified by Z value. The positions of these anomalous values are shown in Pl. I-18.

Range of Z value	Number of measurements	Range of reading values	Multiple of B.G.M.
3 - 4	20	215.2 - 256.4	2.70 - 3.22
4 - 5	11	257.7 - 292.6	3.23 - 3.67
more than 5	23	317.3 - 798.0	3.98 - 10.01

In the literature on exploration results from the radon etch method, many cases indicate anomalous values of 3 - 10 times B.G.M. on the ground surface when there is uranium mineral deposit, extraction of which may be economically feasible at the depth of 100 m from the ground surface. Therefore, it is assumable that reading values more than 3 times B.G.M. in this survey indicate the possibilities of uranium mineral deposits or uranium mineralization.

The Terradex report states that the B.G.M. value of the surveyed area (80 T/sq.mm.30 days) is about a half of values for uranium mineral deposits in many parts of the world. The report suggests that from the anomalous values and their distribution, there is large possibility of the presence of low grade uranium ore deposit at shallow depths and/or high grade uranium mineral deposit at greater depths in the surveyed areas.

(2) Principal Analysis

In the principal analysis, reading values were classified by geology, and these readings were statistically processed (logarithmic conversion) with computer using the accepted method for statistical processing of the Poisson distribution. The results of the statistical processing are listed in Table I-11, and a histogram and accumulated frequency distribution are shown in Fig. I-4. Geological classification of the cup emplacement points is given below. For the purpose of comparison with the results of the Terradex preliminary analysis, the entire area, though not

geologically classified, is discussed.

Group 1 Cups which were emplaced in the area of the Quarternary system

Group 2 Cups which were emplaced in the area of the Tertiary system

Group 3 Cups which were emplaced in the area of the Cretaceous system

Group 4 Cups which were emplaced in the area of β_{P-T} Basalt Formation

Group 5 Cups which were emplaced in the area of P-T Red Sandstone Formation

Group 6 Cups which were emplaced in the area of the Basement

(a) Discussion of All Reading Values (Fig. I-4-1)

The histogram shows an almost conpletely logarithmic normal distribution. The geometrical mean is 75.4 T/sq.mm.30 days. This value is slightly lower than the B.G.M. value in the preliminary analysis. It is reasonable to conclude that the mean of background distribution is 75~80 T/sq.mm.30 days taking also the results of the preliminary analysis into consideration. According to the cumulative frequency distribution diagram, the distribution has no sharp bend and is almost linear. However, it is slightly convex at the point between 160 and 170 T/sq.mm.30 days. This point almost corresponds to that in the preliminary analysis of Z = 2 which is B.G.M. + 2 B. It is considerable that the above point is the threshold value of the reading value distribution when geological considerations are not taken into account. Furthermore, it is acceptable that the readings of which the Z value was 2 to 3 in the preliminary analysis represent anomalous background. In other words, it is assumable that the background mother group and anomalous mother group are both distributed around this point. Therefore, reading values for Z = 3 or more, which have been distinguished as anomalous values in the preliminary analysis,

are considerable to be clear anomalous values when geological considerations of the cup emplacement points are not taken into consideration.

(b) Discussion of Group 1 (Fig. I-4-2)

196 reading values belong to this group, the majority of which are for cups emplaced in the plain in the north of the Zayda Granite Body. In this area, several meters thick soft siltstone covers the P-T Red Sandstone Formation. Emplacement was in this silt formation. The range of reading values was from 4.1 to 798.0 T/sq.mm.30 days. The geometrical mean of these is 98.7 T/sq.mm.30 days (logarithmic value: 1.994) and the standard deviation 0.3088 (logarithmic value). The histogram shows almost normal logarithmic distribution, but the distribution is slightly concentrated in the area in which the mean value is exceeded. In the cumulative frequency distribution, a bend is seen at 237 T/sq.mm. 30 days; this point is the threshold value. Below the threshold value, the geometrical mean value of the background is 85.9 T/sq.mm.30 days (logarithmic value: 1.92) and the standard deviation is 0.2558 (logarithmic value). Of the 196 reading values, there were 19 anomalous values. The anomalous values ranged from 238.1 to 798.0 T/sq.mm.30 days, which are 2.77 to 9.29 times the background geometrical mean.

(c) Discussion of Group 2 (Fig. I-4-3)

126 readings belong to Group 2. The distribution range of reading values was 11.5 to 272.4 T/sq.mm.30 days, of which the geometrical mean is 51.1 T/sq.mm.30 days (logarithmic value: 1.708) and the standard deviation is 0.2861 (logarithmic value). The histogram shows an almost normal logarithmic distribution, however the extent of the tail in the histogram is small. No bend is seen in the cumulative frequency distribution. The threshold value of this group is concluded to be at 190.6 T/sq.mm.30 days which is twice the standard deviation plus the mean value.

The geometrical mean of the background below the threshold value is 49.2 T/sq.mm.30 days (logarithmic value: 1.692) and the standard deviation is 0.2693 (logarithmic value). Three anomalous values larger than the threshold value were observed. These are in the range of 194.7 to 272.4 T/sq.mm.30 days which are 3.96 to 5.54 times the background geometrical mean.

(d) Discussion of Group 3 (Fig. I-4-4)

174 readings belong to this group. The distribution range of reading values was 9.2 to 330.8 T/sq.mm.30 days, of which the geometrical mean is 55.5 T/sq.mm.30 days (logarithmic value: 1.744) and the standard deviation is 0.3034 (logarithmic value). The histogram shows almost normal logarithmic distribution if the unevenness is smoothed out but the distribution is slightly dense in the area exceeding the mean value, as in Group 1. No remarkable bend is seen in the cumulative frequency distribution. The threshold value of Group 3 was determined by the same method as for Group 2. This value is 224.3 T/sq.mm.30 days. For the background below the threshold value, the geometrical mean is 54.0 T/sq.mm.30 days (logarithmic value: 1.732) and the standard deviation is 0.2919 (logarithmic value). Of 174 readings, 3 are anomalous values larger than the threshold value. These values are in range of 224.4 to 330.8 T/sq.mm.30 days which are 4.16 to 6.13 times the background geometrical mean.

(e) Discussion of Group 4 (Fig. I-4-5)

The readings in Group 4 number 27. The distribution range was 16.0 to 176.3 T/sq.mm.30 days. The geometrical mean is 61.9 T/sq.mm.30 days (logarithmic value: 1.791) and the standard deviation is 0.2441 (logarithmic value). Because the number of readings is few, the cumulative frequency distribution is scattered, but the general tendency is nearly linear. The threshold value is 190.2 T/sq.mm.30 days which was determined

by the same way as for Group 2 and 3. All readings are less than the threshold value and no anomalous value is observed.

(f) Discussion of Group 5 (Fig. I-4-6)

The readings of Group 5 number 138. The distribution range was 4.6 to 796.7 T/sq.mm.30 days, of which the geometrical mean is 108.4 T/sq.mm. 30 days (logarithmic value: 2.035) and the standard deviation is 0.3240 (logarithmic value). The histogram of readings shows almost normal logarithmic distribution. The cumulative frequency distribntion is nearly linear, but bend (downward convex) is observed (not so clearly) at 146.3 T/sq. mm.30 days. This point is the threshold value, the same as for Group 1. It is assumable that both mother groups are around this point. For the background below the threshold value, the geometrical mean is 77.5 T/sq.mm.30 days (logarithmic value: 1.889) and the standard deviation is 0.2249 (logarithmic value).

Of 138 readings, there are 38 anomalous values which are larger than the threshold value. This number is larger than that of the other Groups. The anomalous values are in range of 146.5 to 796.7 T/sq.mm.30 days which are 1.89 to 10.28 times the geometrical mean of the background.

(g) Discussion of Group 6 (Fig. 1-4-7)

The readings in Group 6 number 12. The distribution range was 38.5 to 429.0 T/sq.mm.30 days, of which the geometrical mean is 117.0 T/sq.mm. 30 days (logarithmic value: 2.068) and the standard deviation is 0.3153 (logarithmic value). The distribution pattern in the histogram is not clear because of the small number of readings. The cumulative frequency distribution is almost linear. The threshold value is 499.6 T/sq.mm.30 days which was determined by the same way as for Group 2, 3 and 4. All reading values are below the threshold value and no anomalous value is observed.

(3) Results of Analysis and Their Relationship to the Geology

The number of anomalous values calculated as explained in the above discussion total 63. This number exceeds that of the anomalous values in preliminary analysis by 9.

When comparing anomalous values from preliminary and principal analysises, most of the values coincide with each other. The number of values which are anomalous in the preliminary analysis but are not anomalous in the principal analysis is 3 in Group 1 and 3 in Group 6 (6 in total). The number of values, not anomalous in the preliminary analysis but anomalous in the principal analysis, is 1 in Group 3 and 14 in Group 5 (15 in total). These anomalous points are shown in Pl. I-18.

The geometrical mean and standard deviation, in Table I-11, which indicate features of the distributions of the readings, can be explained as follows.

For all readings including anomalous ones in each group, the standard deviations are within 0.3 ± 0.02 (logarithmic values) except that in Group 4, and dispersions after logarithmic conversion are assumable to be almost the same. The standard deviation, for Group 4, is 0.24, and the dispersion is smaller than for the other groups. The geometrical mean except for Group 1 is largest for Group 6. It lessened successively from Group 6 to Group 2, being the smallest for Group 2. This fact exactly corresponds to the results of the first phase geological survey, that radioactivity was fell successively from basement rock to the Quaternary system. Group 1 is ranked next to Group 5. readings of Group 1 were mostly obtained in Q_2 Silt Formation which thinly covers P-T Red Sandstone Formation. It could be considered that these values were influenced by this P-T Red Sandstone Formation.

For the background from which anomalous values have been eliminated,

the tendency of the geometrical mean is similar to that for each Group. However, the standard deviation has wide range from 0.24 to 0.315 because of the differences in the threshold values. The dispersion is smallest for Group 5 and rather large for Groups 2, 3 and 6.

From the above point of view, has been assumed that P-T Red Sandstone Formation contains uniformly more uranium than other formations, except the basement rock. The high reading values could suggest that there would be uranium mineralization. For other formations, the newer the age of the formation is, the smaller the uranium content becomes. The fact which the dispersion range was larger than that of P-T Red Sandstone Formation suggests that uranium existed locally or have been influenced by P-T Red Sandstone Formation and Basement or uranium ore deposits contained in them. Basement rocks generally contain more uranium than sedimentary rocks, but uranium mineralization may be local and not uniform.

(4) Relationship Between Radioactivity and Radon Etch Readings

Radioactivity was measured at each point of emplacing radon detector cups. For the purpose of reviewing the correlation, radon gas reading and radioactivity have been converted into logarithmic values. The results are as follows.

	Correlation: radioactivity/radon etch reading
Group 1	0.390
Group 2	0.503
Group 3	0.407
Group 4	0.103
Group 5	0.315
Group 6	0.044
All measuring points	0.524

Pl. I-20 shows the relationship between the radon etch readings, radioactivity and geology. As shown in Pl. I-20, there is no clear relationship between the radioactivity and radon etch readings. From the above, it is assumable that the reading values indicate not only shallow uranium but also rather intense reaction from deep uranium.
It is considerable that anomalous values, especially, do not indicate shallow uranium concentrations, but indicate those of depths.

(5) Contour Map

For the purpose of reviewing the survey results, in addition to the extraction of anomalous values, contour map was prepared by the 5-point weighted-average method to show the distributing tendency of readings. This map is shown in Pl. I-19.

This contour map accompanied the Terradex preliminary report. The map was prepared with separate values calculated from actual readings for the entire surveyed area. In the method, reading values of 5 points which are nearest to the point to be calculated are weight-averaged by using the reciprocal of the distance. The general formula is as follows:

$$eXj = \frac{\frac{1}{ri-j} \cdot Xi}{\frac{1}{ri-j}}$$

where: i = 1, 2, 3, 4 and 5

Xi = reading value at point i

eXj = calculated value at point j

ri-j = distance between points i and j

Contours drawn on the basis of eXj values indicate rather truly the distribution of actual reading values. In addition to the above method, there are other methods, using 6 points (i = 1 ~ 6), 8 points (i = 1 ~ 8), etc. However, Terradex state that the 5-point method is most suitable

for the analysis of sedimentary formation area.

2-2-3 Anomaly Area

(1) Distribution of Anomaly

Anomalies were almost distributed in the north of Zayda Granite Body, however some were observed in the area from the north of Zayda to the north of Bou Mia Granite Body.

In the north of the Zayda Granite Body, large concentration of anomalies was observed in the north of Immayn-Ait-Rahhou (the same observation is made in both the preliminary and principal analyses). In addition to the above, concentration of 4 to 5 anomalies is seen in the north of Assaka-n-Tabhirt, that of 8 to 9 anomalies in Idamrane Micha and few anomalies (in the principal analysis) in the northeast of Zayda and Ilaghmane-n-Amar.

In the area from the north of Zayda to the north of Bou Mia Granite Body, there are scattering only 6 to 7 anomalies (both preliminary and principal analyses). The neighbouring 2 anomalies (in the principal analysis) near Zayda attract attention.

(2) Contour Map

The contour map shows vary high value area of the anomaly concentration in the north of Immayn-Ait-Rahhou and small sized high-value area in the north of Assaka-n-Tabhirt located in the west of Immaya-Ait-Rahhou. These two high-reading-value areas tend to extend to the northwest. In Idamrane-Micha, areas of 200 ~ 250 T/sq.mm.30 days are observable around the anomalies. These indicate slight tendency to extend NE-SW and NW-SE. In other areas, anomalous areas are scattered, such as 150 T/sq.mm.30 days (N-S) in Tirouwadine in the north of Bou Mia Granite Body, 150 T/sq.mm.30 days (E-W) in Izatimane, 175 T/sq.mm.30 days in the southeast of Ait Bassou, 175 T/sq.mm.30 days in Ilighname Sidi Middah, etc.

(3) Relationship Between Anomalous Area, Geology and Geological Structure

The area which greatly attracts attention is the area of remarkable anomalies concentration located in the north of Immayn-n-Ait Rahhou. In this location, there are anomalies about 10 times B.G.M. or geometrical mean of the background. This location is equivalent to northeastern extension of the vein-like type uranium concentration area around Pancau-1. There are many anomalies in the area from the north of Assaka-n-Tabhirt to the east of Idamrane Micha, compared with other areas, and the high value areas are very clear on the contour map. This area consists of P-T Red Sandstone Formation covered with thin Quaternary Formation. From the ground surface to the basement is as shallow as 50 ~ 60 m. The palaeo-currents on the basement rock, which were clarified by gravity survey, flows northward from Immayn-n-Ait Rabhou, Peneau-1, Assaka-n-Tabhirt, etc. Anomalous areas determined by the radon etch survey agree with the geological structure of the above area. Therefore, it has been considered that the radon etch anomalous areas suggest the existence of uranium mineral deposits or uranium mineralization.

Except from the above areas, anomalies are about 3 times B.G.M. and several times the geometrical mean of the background, that is, the values are rather low and the locations are scattered. In such areas, P-T Red Sandstone Formation is exposed, as in the north of Zayda, and palaeo-currents are estimated on basement rocks. Therefore, geological conditions are similar to those of Immayn-n-Ait Rahhau. In the most parts of such areas, Cretaceous or younger systems is distributed, and P-T Red Sandstone Formation, in which uranium mineralization could be expected to be, is at greater depths. Where P-T Red Sandstone Formation is exposed, as seen in the north of Zayda, there is little possibility of the existence of uranium mineral deposits in terms of the results of the radon etch survey. In

the area where Cretaceous or younger systems are distributed, there could be the possibility that high anomalous area was not detected because the lower part of P-T Red Sandstone Formation is much deep below the surface.

From this point of view, it should be worth noting that several anomalies were detected closely in the north of Bou Mia granite.

(4) The Radon-etch Method and Future Programme

Spacing of radon detector cups was as wide as 500 m and 1,000 m in this survey. By combining the results of gravity prospecting and geological surveying, the north area of Immayn-n-Ait Rabhou has been selected as the most probable uranium mineral deposit area. The existence of a high quality uranium mineral deposit cannot be clarified without a further detailed survey. However, it is noteworthy that combination of the Radon Etch method and other prospecting methods has proved much effective for the identification of the area to be detailed surveyed in the future.

In the future survey programme, it will be necessary to employ 50 m ~ 200 m cup spacings in the selected anomalous areas that is, from the north of Assaka-n-Tabhirt to the east of Idamrane Micha, and also that the possibility of uranium mineral deposits and uranium mineralization must be elucidated by comprehensive review of the results of to detailed survey of geology and prospecting by drilling in addition to the previous results of geological surveys and gravity survey.

PARTICULARS

PART II

Geophysical Survey

PART II GEOPHYSICAL SURVEY

Chapter 1 General Description of Survey ..... II- 5

1-1 Summary ..... II- 5

1-2 Outline of Topography and Geology ..... II- 5

Chapter 2 Gravity Survey ..... II- 9

2-1 Gravity Observation II-10

2-2 Corrections of Gravity Values II-12

2-3 Method of Analysis II-17

Chapter 3 Survey Results II-30

3-1 Bouguer Anomaly Map II-31

3-2 Regional Gravity Trend Maps II-33

3-3 Residual Gravity Map in Polynomial of the Second Order II-36

3-4 Intermediate Wave-Length Bouguer Anomaly Map II-39

Chapter 4 Underground Structure Estimated from Survey Results II-42

4-1 Correlation between Gravity Distribution and Geology II-43

4-2 Contour Line Map of Depth from Ground Surface to Basement Rocks II-46

4-3 Profiles of Underground Structure II-48

4-4 Interpreted Map of Underground Structure II-52

4-5 Conclusion II-57

List of Illustrations

Fig. II-1	Location of Gravity Survey (1 : 200,000)
Fig. II-2	Sketches of Gravity Base Stations
Fig. II-3	Network of Leveling Survey (1 : 200,000)
Fig. II-4	Grids of Topographical Correction
Fig. II-5	Geological Map and Locality of Rock Samples (1 : 200,000)
Fig. II-6	Gravimetric Value-Elevation Curve
Fig. II-7	Correlation between Bouguer Anomaly Values and Station Altitude
Fig. II-8	Bouguer Anomaly Map on Haute Moulouya Area (1 : 500,000)
Fig. II-9	Compiled Bouguer Anomaly Map (1 : 200,000)
Fig. II-10	Regional Gravity Trend in Polynomial of Second Order (1 : 200,000)
Fig. II-11	Regional Gravity Trend in Polynomial of Third Order (1 : 200,000)
Fig. II-12	Residual Gravity Map in Polynomial of Second Order (1 : 200,000)
Fig. II-13	Intermediate Wave-Length Bouguer Anomaly Map (1 : 200,000)
Fig. II-14	Contour Line Map of Depth from Ground Surface to Basement Rocks (1 : 200,000)
Fig. II-15	Profiles of Underground Structure (1 : 200,000)
Fig. II-16	Interpreted Map of Underground Structure (1 : 200,000)

List of Tables

Table II-1	Calculation of Gravity Values at Base Stations
Table II-2	Densities of Rock Samples
Table II-3	Distribution of Rock Densities

Appendices

Table II-4	Earth Tide Correction and Drift Correction
Table II-5	Topographical Correction
Table II-6	Altitude Correction and Latitude Correction
Table II-7	Photographs

List of Plates (1 : 50,000)

Pl. II-1	Locations of Gravity Stations and Their Altitudes
Pl. II-2	Bouguer Anomaly Map ($\rho = 2.5$)
Pl. II-3	Residual Gravity Map in Polynomial of Second Order
Pl. II-4	Intermediate Wave-Length Bouguer Anomaly Map
Pl. II-5	Contour Line Map of Depth from Surface Ground to Basement Rocks
Pl. II-6	Profile of Underground Structure A - B
Pl. II-7	Profile of Underground Structure C - D
Pl. II-8	Interpreted Map of Underground Structure

Chapter 1 General Description of Survey

1-1 Summary

1-1-1 Purpose

This report is about gravity measurements and their interpretation in Haute Moulouya, the Kingdom of Morocco. Main purposes of the survey are to realize the subterranean geological structure -- mainly structure of a basement -- of district under survey, to understand geological environments and the likely deposits of, mainly, lead and uranium ores and to set guidelines for further exploration.

1-1-2 Location and Scope

The district under survey is in a steppe surrounded by the mountains of Moyen Atlas and Haut Atlas in the central part of the Kingdom of Morocco and, administratively, included in the county of Midalt.

This district, as indicated in Fig. II-1 (Location of Gravity Survey), is on the north side of Zayda and covers about 400 km² ranging lat. 32°49' to 32°58' N and long. 4°41' to 5°07'W.

1-1-3 Period

The period of the field survey and analysis in Japan were as follows:

Gravity survey	May 21 - July 3, 1979
Leveling	May 21 - July 5, 1979
Field analysis	June 28 - July 12, 1979
Total period of field survey	May 15 - July 18, 1979
Analysis in Japan	July 19, 1979 - February 20, 1980

1-2 Outline of Topography and Geology

1-2-1 Topography

The surveyed area is located in the northwestern part of the basin

held between the mountains of Moyen Atlas and Haut Atlas. The Moyen Atlas mountains are peneplain-like with an altitude of about 2,000 m and run in the direction of NE-SW. The Haut Atlas mountains include peaks of over 3,000 m in elevation and run in the direction of NEE-SWW.

The surveyed area is generally of gentle hills, except for the central and western parts where platforms exist sporadically. In the western part of the surveyed area adjoining the Moyen Atlas, the elevation which is some 1,800 m gradually decreases in the eastern direction to be about 1,300 m at the east end of the surveyed area. With an average slope of less than 1°, the topography is generally flat.

The Moulouya river flowing east from the south end of the surveyed area to the southeastern part outside the area is the trunk of the local river system. Also, small rivers and valleys running in the direction of N-S or NE-SW are developed -- notably the Bouhafce, Bou La'joul and Sidi Ayyad rivers which are tributaries of the Moulouya river. Some marshes exist in the eastern half of the surveyed area.

There are no remarkable erosions, tali or terraces in this area, except for the small tali found in the watersheds of the main rivers. However, the Moulouya river flowing through the southeastern part outside the surveyed area is greatly eroded and forms deep valleys.

1-2-2 Outline of Geology

The outline of the geology in the surveyed area is as follows (see Fig. II-5, Table II-3):

The basement rocks in this area are composed of Precambrian or Palaeozoic crystalline schists and the Granites intruding into them. There are outcrops of the so-called Zayda Granite Body on the southern edge of the surveyed area. The Granites are composed of porphyritic granite, aplitic granite, granodiorite and contaminated granite and these apparently

form most of the basements in this surveyed area. Meanwhile, crystalline schists occur slightly on the ground surface at the eastern end of the surveyed area but, to the east of the surveyed area, there is a large known occurrence of crystalline schists adjacent to the Zayda Granite Body.

These basement rocks are covered -- from the base upward -- with Permo-Traiassic P-T Red Sandstone Formation and β_{P-T} Basalt Formation, Cretaceous Cenomanian K_{2cm} Mudstone Formation and Turonian K_{2t} Limestone Formation, Tertiary T_1 Mudstone Formation·T_2 Marl Formation·T_3 Sandstone Formation, and Quaternary Q_1 Siltstone Formation·Q_2 Siltstone Formation· Q_3 River Sediments. These are accumulated in a gentle slope which is almost level. Also, Quaternary β_{Q_2} Basalt lava flows on a small scale.

The main geological stratigraphy greatly differs between the eastern half of the surveyed area and its western half. In the eastern half, P-T Red Sandstone Formation, β_{P-T} Basalt Formation and K_{2cm} Mudstone Formation lie in ascending order in the northern direction, showing an E-W distribution. Further, Q_2 Siltstone Formation which unconformably covers these extends over a large area and there is hardly seen any surface occurrence of K_{2t} Limestone Formation, T_1 Mudstone Formation and T_2 Marl Formation and T_3 Sandstone Formation.

In the western half of the area, P-T Red Sandstone Formation, K_{2cm} Mudstone Formation, K_{2t} Limestone Formation, T_1 Mudstone Formation, T_2 Marl Formation and T_3 Sandstone Formation conformably lie in ascending order in the western direction, showing a NNE-SSW distribution along the topographical elevation. Characteristically, there is no surface occurrence of β_{P-T} Basalt Formation.

As for fault structure, NE-SW or NNE-SSW faults are identified at the

west end of the surveyed area. Faults in the direction of NE-SW with fracture zones are remarkable in the area extending from the southern part of the surveyed area to its eastern part, particularly about the Zayda Granite Body. Larger of these fault groups are presumed to interrupt the underground occurrence of basement rocks.

Chapter 2 Gravity Survey

This chapter is about measurements, data reduction and analysis of this gravity survey. All procedures from field survey to report preparation are indicated in the following flow chart:

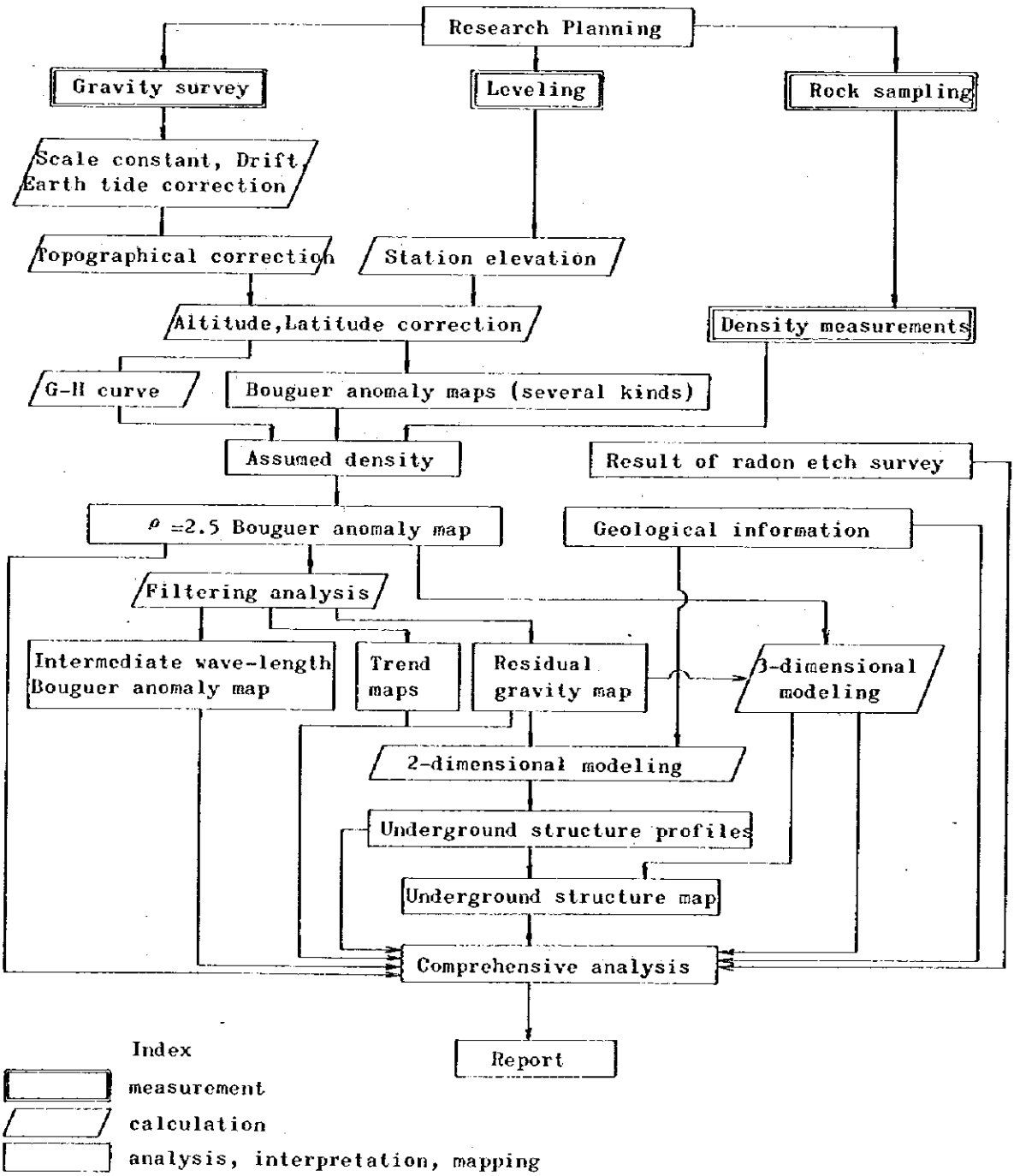

2-1 Gravity Observation

2-1-1 Gravity Meter

Gravity values were measured, using two gravity meters, one numbered G-236 and the other G-366, produced by La Coste & Romberg INC. These gravity meters have a reading scale of 0 to 7,000 and can measure gravity values ranging from 0 mgal to about 7,300 mgal.

The gravity value conversion table for these gravity meters is partially shown below:

Counter Reading	Value in Milligal		Factor for Interval	
	G-236	G-366	G-236	G-366
2500	2658.64	2643.38	1.06430	1.05787
2600	2765.07	2749.17	1.06438	1.05796
2700	2871.51	2854.96	1.06445	1.05805
2800	2977.96	2960.77	1.06451	1.05813
2900	3084.41	3066.58	1.06456	1.05821
3000	3190.86	3172.40	1.06460	1.05829

2-1-2 Gravity Stations

Details of the stations used in this gravity survey are as follows:

Surveyed area	Approx. 400 km²
Station-to-station interval	Approx. 400 m
Number of stations	878 stations

The gravity stations were numbered by their localities as follows:

Sub-base station	No. 2001	1 station
Main road	No. 1 - 175	175 stations
Northwestern part	No.201 - 281	81 stations

Southwestern part	No. 301 - 465	165 stations
Central part	No. 501 - 683	183 stations
Eastern part	No. 701 - 775 No. 801 - 998	273 stations
Total		878 stations

The positions of gravity stations were selected in consideration of anticipated basement depths. Short station-to-station intervals and high station denseness were used in areas with presumably shallow basements and long station-to-station intervals and low station denseness were used in areas with presumably deep basements.

The positions of gravity stations were decided by referring to roads, rivers, structures and topographical features on topographical maps. Where reliable topographical features for determination of a station position were lacking, positions for such stations were determined with distance measurements such as stadia survey using automatic levels, chain measuring and pacing, and with bearing measurements using compass.

2-1-3 Standard of Gravity Values

The gravity value of 979,154.65 mgal at gravity datum point B-7 which was established during the geophysical prospection (Prospection Geophysique par Procede de Gravimetrie et Magnetometrie Dans les Bassins de la Moyenne Moulouya de la Haute Moulouya et D'itzer Engil, Solaini L. 1965) was used as the standard value of this survey.

Base station No. 1000 was set up in front of the staff quarters in Itzar as a base station for closed observation. Fig. II-2 shows the positional relationship of these gravity base stations.

As indicated in the appended Table II-1, the gravity value at the base station No.1000 was decided by closed observation involving two round trips from gravity datum point B-7. The mean value of 979,126.533 mgal

from the two observations was employed as the standard gravity value for the closed measurement carried out once a day.

2-1-4 Leveling

Leveling was performed, using three B-2 automatic levels, products of Sokkisha Co. Elevation 1,458.78 m at the above-mentioned gravity datum point B-7 and elevation 1,801.92 m at B-8 were employed as standard elevations.

As indicated in Fig. II-3 (Network of Leveling Survey), the survey was taken by closed routes insofar as possible to increase accuracy.

The closing errors for each route, in the appended calculating tables, completely satisfy the following specification:

closing error : $\varepsilon \leqq 100\sqrt{D}$ mm (D: distance of closed route in km)

Elevations of every stations are shown in Pl. II-1 (Locations of Gravity Stations and Their Altitudes).

2-2 Corrections of Gravity Values

Observed gravity values are affected by many factors, such as time, location, elevation, and relative topography, etc. at each station. In order to correct these factors and to get gravity values under the same condition, the following corrections were performed. These corrections were carried out by an electronic computer.

2-2-1 Drift Correction

It is usual to show different gravity value compared to the gravity value which is measured a few hours before, even if earth tide correction is done for both values. This typical error of a gravity value is called drift of a gravity meter and its variation rate can be corrected by assuming that it varies linearly to time.

In Table II-4 on the appendices, drift rates per day and per hour satisfy the specification of 0.2 mgal/day.

2-2-2 Earth Tide Correction

Earth tide correction is to eliminate influence of location change of the moon and the sun affecting on gravity observation. Influence of the sun and the moon varies with time, latitude, and elevation of an observation station. By applying this correction, an accuracy of observation can be improved, because drift correction value is detected as a simple closing error.

Earth tide correction value (Δg) is as follows:

$$\Delta g = 1.2 \left\{ \frac{3}{2} r_0 \cdot \frac{M}{E} \cdot \frac{a}{r^3} \cdot \rho^2 \left\{ \cos^2\phi \cdot \cos^2\delta \cdot \cos 2\theta + \sin 2\phi \cdot \sin 2\delta \cdot \cos\theta + 3.0 \left(\frac{1}{3} - \sin^2\phi \right) \left(\frac{1}{3} - \sin^2\delta \right) \right\} \right]$$

where

r_0 = 978.049 (1 + 0.0052884 $\sin^2\phi$ - 0.0000059 $\sin^2 2\phi$) gal

ϕ : latitude of the station

δ : astronomical declination

θ : astronomical hour angle

ρ : mean radius of the earth (6370.28 Km)

r : distance from the earth's center to the sphere

sun: 1,496 × 10^8 Km

moon: 384,405 Km

a : distance from the earth's center to the station

= 6378.388 (0.99832 + 1.6835 × 10^{-3} cos 2ϕ - 3.5 × 10^{-6} cos 4ϕ)

+ elevation at the station (Km)

$\frac{M}{E}$: mass ratio of the sphere and the earth

(sun:332958 ; moon:0.0123)

2-2-3 Topographical Correction

Topographical correction is a correction to eliminate influence to a

gravity value of irregularities of surrounding topography. Topographical maps are divided by grids of an equal spacing and the elevations at the center of each grid are read to know relative undulation among observation stations. Gravity values affected by each block separated by grids are summed up to get a topographical correction value of a concerned observation station.

Topographical influence by these blocks becomes bigger as distance of a block to a station is nearer and becomes smaller as distance to a station is further. Based on this phenomena, highly precise topographical correction was carried out for an area near to station, while rough correction was carried out for a remote area.

Scales of topographical maps, ranges of correction and grid spacings for each correction are as follows:

	Far	Middle	Near	Adjacent Area
Scale of Map	1/100,000	1/50,000	1/50,000	
Correction range (N - S)	120 Km	24 Km	4 Km	20 m radius
Correction range (E - W)	120 Km	24 Km	4 Km	20 m radius
Grid spacing	4000 m	1000 m	250 m	

Relation between grids and a station is shown in the appended Fig. II-4 (Grids of Topographycal Correction).

Each correction calculations were done by an electronic computer. Following Kane's formula is used for each correction in Far, Middle, and Near areas.

Kane's formula is

$$g = 2G\rho A^2 (R_2 - R_1 + \sqrt{R_1^2 + H^2} - \sqrt{R_2^2 + H^2}) / (R_2^2 - R_1^2)$$

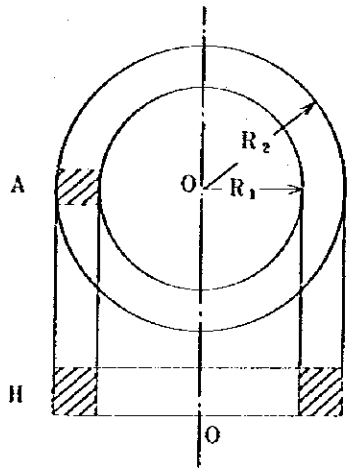

g : topographical correction value

G : gravitational constant

ρ : density

R_1 : distance from the station to inside of grid

R_2 : distance from the station to outside of grid

A : length of correction block

H : height of correction block

However, correction of a block including a station can be caluclated by assuming a head cut pyramid which is drawn by connecting elevations of adjacent blocks and the station (center) elevation with straight lines and eliminating an area within 20 m from the station. This relation is shown in the following schematic diagram:

R : near grid distance (250 m)

r : adjacent correction range (20m)

ΔH : elevation difference between blocks

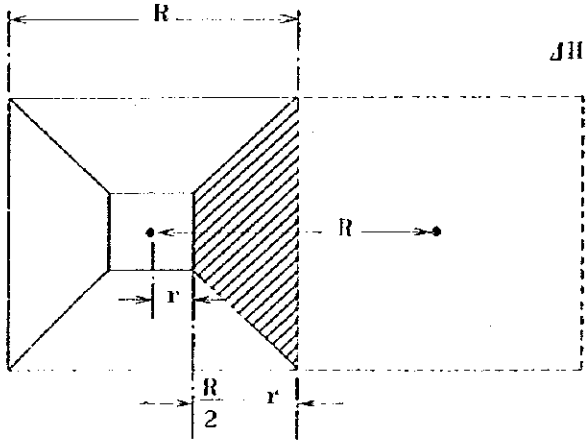

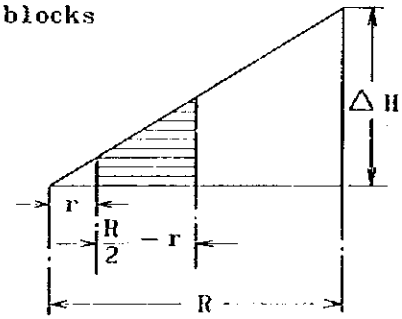

For adjacent correction within 20 m from the station, cross section was drawn and correction value is calculated by the following formula:

$$\Delta g = 2G\rho H\left(\tan^{-1}\frac{2(D+A)}{H+2L} - \tan^{-1}\frac{2D}{H+2L}\right)$$

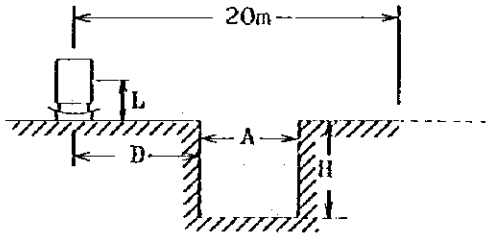

Δg : correction value for adjacent topography

G : gravitational constant

ρ : density

L : gravity meter height (0.2 m)

2-2-4 Altitude Correction

An altitude correction includes a free air correction which is a correction of gravity value due to simple elevation difference and a Bouguer correction due to attraction of underground rock density.

A free air correction value Δg_1 is calculated by the following formula using the mean vertical gravity gradient of the earth's surface.

$$\Delta g_1 = g_0 \left\{ 1 - \frac{R^2}{(R+H)^2} \right\} = \frac{2g_0 HR + g_0 H^2}{(R+H)^2} \simeq \frac{2g_0}{R} H \fallingdotseq 0.3086H \text{ mgal}$$

where

g_0 : gravity value at geoid

R : mean radius of the earth (m)

H : elevation of a station (m)

A Bouguer correction Δg_2 is calculated by the following formula, providing that an infinite slab having a thickness H and a density ρ exists between the geoid and the earth's surface.

$$\Delta g_2 = -2\pi G\rho H \fallingdotseq -0.0419\rho \cdot H \text{ mgal}$$

where

G : gravitational constant

ρ : density

H : elevation of a station (m)

A free air correction and a Bouguer correction are functions of elevation of a station. Therefore, they can be added together into the following formula:

$$\Delta g_1 + \Delta g_2 = (0.3086 - 0.0419\rho) H \text{ mgal}$$

and called an altitude correction.

2-2-5 Latitude Correction

Shape of the earth is not perfectly spherical but an oblate spheroid and a gravity value on the surface of the earth is minimum around the equator and becomes maximum at both poles due to oblate shape and centrifugal force of rotation of the earth. The international gravity formula gives the standard gravity value S.V. as follows:

$$S.V. = 978{,}049\ (1 + 0.0052884\ \sin^2\phi - 0.0000059\ \sin^2 2\phi)\ \text{mgal}$$

This also gives a correction of latitude ϕ of each station.

2-3 Method of Analysis

In the following paragraphs analytical process of the survey will be explained, by using a Bouguer anomaly map which was drawn by using previously mentioned corrections on observed gravity values.

2-3-1 Density Measurements of Rock Samples

A gravity anomaly reflects a density contrast in underground. Therefore, it is necessary to find average densities of rocks and density distributions of layers in the surveyed area in order to analyze underground structure from gravity anomalies.

In this survey, density measurements were carried out on 93 rock samples collected. We also studied the results of density measurements of rock samples in Haute Moulouya region. (La Structure en Profondeur de la Region de la Haute Moulouya D'apres les Donnees Geophysiques, Tchernysh G. 1977)

These results are listed in Table II-2 (Densities of Rock Samples) and Fig. II-5 (Geological Map and Locality of Rock Samples) and consolidated in Table II-3 (Distribution of Rock Densities) along with the results of rock density measurements in the previous year to facilitate comparison

with representative formations in the surveyed area.

For density measurements, rock samples were soaked in water then wiped off excessive water in order to obtain condition where rock samples were in the underground. Rock density was calculated from the following formula:

Density : $\rho = \frac{Wa}{Wa - Ww}$ Wa : weight in air

Ww : weight in water

Special attention was paid while collecting rock samples. Only fresh rock samples were carefully collected and the samples were collected from every formation in the surveyed area shown in Table II-3. An average density of each formation does not necessarily represent the formation density itself but a general tendency of density difference is considered to be obtained.

The followings may be considered from the results of density measurements of rock samples. The names and marks of geological formations used in the charts are based on the classification used in the geological survey of the current year.

(a) The densities of all rock samples range widely from 1.81 to 3.09. Particularly, those of Quaternary and Tertiary rocks greatly vary, reflecting the difference of density by modes of occurrence. Whereas, the densities of rocks in the Cretaceous and older formations scarcely vary. This is particularly the case with the Granites.

(b) The average density of 2.78 for Quaternary β_{Q_2} Basalt lava and the average densities of 2.60, 2.70 and 2.79 for, respectively, Granites, granodiorite and crystalline schists which form basement rocks may be mentioned as belonging in the high density group. Of these, β_{Q_2} Basalt lava is very close and has immense density but is thought to occur only locally and be thin; thus it is unlikely seriously to affect to the gravity

anomalies.

(c) Of the basement rocks, crystalline schists occurred on the ground surface at the east end of the surveyed area indicate especially high densities and presumed to be conducive to remarkable high-gravity anomalies. As for granodiorite, this intrudes only partially to the east of the surveyed area and seems scarcely to affect to the gravity anomalies in this area.

(d) The Granites believed to form the basement in the most part of the surveyed area -- including aplitic and contaminated types -- have stabilized high densities averaging at about 2.6.

(e) As the average densities for sedimentary formations covering basement rocks, there are 2.33 for Quaternary, 2.39 for Tertiary, 2.48 for Cretaceous, 2.40 for Jurassic and 2.48 for Permo-Triassic. As a whole, these formations may be considered to be of low densities, the average being about 2.4.

(f) From the above, the densities of layers in this area may be generally divided as follows:

Upper low-density formations		$\rho = 2.4$
Basement rocks	Granites	$\rho = 2.6$
	Crystalline schists	$\rho = 2.8$

Since the Granites occur the most part of the basement in the surveyed area, a two-layer structure with a density difference of about 0.2 between the Granites and the upper low-density formations described in (e) may be assumed for places where the Granites form the basement. However, a high-density third layer must be anticipated for areas with the occurrence of crystalline schists and the vicinities and analysis by a two-layer structure is inapplicable to such areas.

2-3-2 Assumption of Correction Density

The results of analysis are greatly affected by assumption of density in the gravity calculations. Results of density measurements of rock samples shown in Table II-3, indicate rock densities near the ground surface between 1.81 and 3.09, but it is not appropriate to determine an average density of each formation, only from measured density values of rock samples collected from the surface of the ground, because a density of a formation changes its density depending on its depth.

Therefore, in this gravity survey, the followings were studied to determine density for gravimetric corrections.

(a) Bouguer anomaly maps were prepared with varying density to four different values (ρ = 2.00, 2.30, 2.50, 2.67) which are essential for topographical correction and altitude correction. Based on four Bouguer anomaly maps prepared, correlation between shape of gravity distribution by these correction densities and topography for each map were examined. It was considered to be proper to adopt Bouguer anomaly map based on a density between ρ = 2.30 and ρ = 2.50.

(b) Average densities of rock samples from each formation, which are thought to represent rocks of the surveyed area, are given as follows:

Sedimentary rocks	Quaternary	ρ = 2.33
	Tertiary	ρ = 2.39
	Upper Cretaceous	ρ = 2.48
	Lower Jurassic	ρ = 2.40
	Permo-Triassic	ρ = 2.48

Basement Complex	Granites	$\rho = 2.60$
	Granodiorite	$\rho = 2.70$
	Crystalline Schists	$\rho = 2.79$
Average density of all rock samples		$\rho = 2.51$

(c) As shown in the appended Fig. II-6 (Gravimetric Value-Elevation Curve), an appropriate correction value of $\rho = 2.48$ was obtained from the relation between the elevations and the gravity values at each station.

(d) The correlation between topographical change using station elevations and Bouguer anomaly values by several types of correction densities is shown in the appended Fig. II-7.

Generally, on the assumption of homogenous underground density, the density at which the Bouguer anomaly profile is even against the unevenness of the topographical profile is considered the appropriate correction density. If the correlation shown in Fig. II-7 is observed from this point of view, correction densities of $\rho = 2.30 \sim \rho = 2.40$ are considered to be appropriate. But if the underground density is not homogenous -- if, for example, a high-density basement underlies at a shallow underground level -- Bouguer anomaly should be high at a low station elevation because of closeness to the basement but it should be low at a high station elevation because of distance from the basement. The correction density is most appropriate when the Bouguer anomaly is $-0.0419 \cdot \Delta\rho \cdot \Delta H$ mgal for $\Delta\rho(g/cm^3)$, density difference of the basement, and ΔH (m), elevation difference.

As the result of review of Fig. II-7 from this view-point, correction density of approximately $\rho = 2.5$ was considered appropriate.

It was decided that analysis was conducted using a Bouguer anomaly map with a correction density of $\rho = 2.5$ and by referring to the above.

2-3-3 Trend Analysis

Shown in detail in Chapter 3, the Bouguer anomaly map shows a remarkable long wave-length trend that seems to be due to isostasy and a large-scale geological structure and it is extremely difficult directly to compare the gravity distribution in the map and the geological structure. Therefore, trend analysis was carried out to eliminate this gravity trend.

The Bouguer anomaly map ($\rho = 2.50$) was divided into grids at intervals of 500 m and the gravity values at each grid point were read. These gravity values at grid points were regarded as a function, G (X, Y), of grid-point positions (X, Y), and a trend of the second order Z_2 (X, Y) and a trend of the third order Z_3 (X, Y) were obtained by the least square method. A map of the regional gravity trend in polynomial of the second order (Fig. II-10) and a map of the regional gravity trend in polynomial of the third order (Fig. II-11) were prepared, based on these. Further, a residual gravity map in polynomial of the second order (Pl. II-3, Fig. II-12) was prepared by subtracting the trend values of the second order from Bouguer anomaly values at each grid point.

The positional relation of the system of X and Y coordinates and the formulae for the trends are as follows:

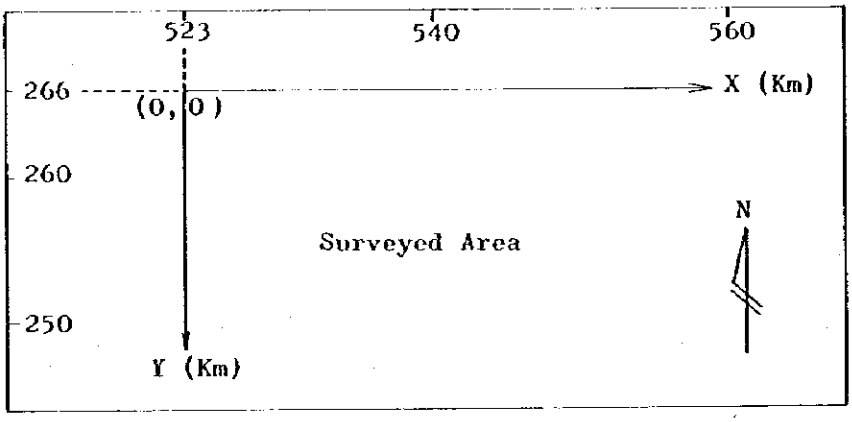

Trend of second order : $Z_2 (X, Y) = -79.867 - 0.87976X - 1.86874Y + 0.00852X^2 + 0.0294 X \cdot Y + 0.01928Y^2$

Trend of third order : $Z_3 (X, Y) = -73.158 - 1.0026X - 3.30226Y - 0.00176X^2 + 0.07204 X \cdot Y + 0.101Y^2 + 0.00024X^3 - 0.00056X^2 \cdot Y - 0.00040 X \cdot Y^2 - 0.00168Y^3$

Residuals of second order = $G(X, Y) - Z_2 (X, Y)$

2-3-4 Wave-Length Analysis

Wave-length gravity values were filtered by the running average method to detect gravity anomalies of several wave-lengths in a Bouguer anomaly map.

Wave-length gravity values for three types: noise, normal and local, by wave-lengths, were calculated, using grid-point gravity values from the Bouguer anomaly map by the following formulae:

$$\text{Noise} = g_0 - \frac{1}{6} \sum_{i=-1}^{1} (g_{xi} + g_{yi})$$

$$\text{Normal} = \frac{1}{6} \sum_{i=-1}^{1} (g_{xi} + g_{yi}) - \frac{1}{14} \sum_{i=-3}^{3} (g_{xi} + g_{yi})$$

$$\text{Local} = \frac{1}{14} \sum_{i=-3}^{3} (g_{xi} + g_{yi}) - \frac{1}{30} \sum_{i=-7}^{7} (g_{xi} + g_{yi})$$

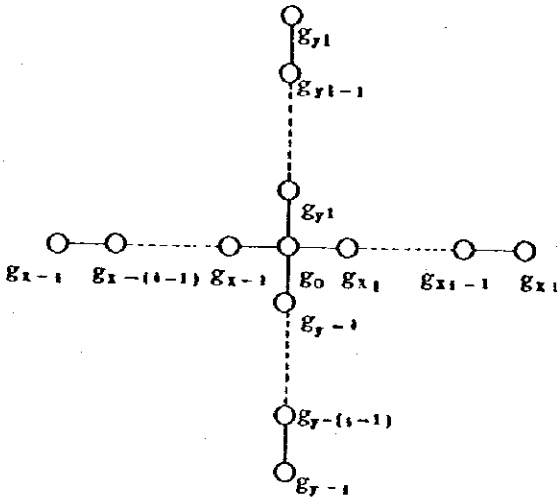

In this survey, "normal" for detecting intermediate wave-length was employed as an intermediate wave-length Bouguer anomaly map (Pl. II-4, Fig. II-13).

2-3-5 Two-Dimensional Analysis

Estimating an underground structure that corresponds to gravity anomaly, two-dimensional modeling calculations on two sections were carried out using residual gravity values of the third order. The results of modeling are drawn as underground structure profiles.

An underground structure model is represented by several polygons and their densities. Gravity values on the surface of the ground induced by the underground structure model were calculated. Then calculated gravity values were compared with gravity values read every 500m on a residual profile. Then, if the coordinate points composing polygons and their densities are regarded as variables, and if these variables are changed, polygonal density models are obtained by least square fitting until calculated gravity values coincide with the residual values.

To calculate gravity values of a polygonal density model, Talwani's method is employed.

A vertical component (gv) of gravity value at point (0), induced by a polygon (infinitely long to the direction perpendicular to this paper) with density ρ on the figure, is given by the following formula:

$$gv = 2\rho G \sum_{i=1}^{n} \int_{z_i}^{z_{i+1}} \int_{\infty}^{x} \frac{z}{x^2 + z^2} \, dx \cdot dz$$

where

ρ : density

G : gravitational constant

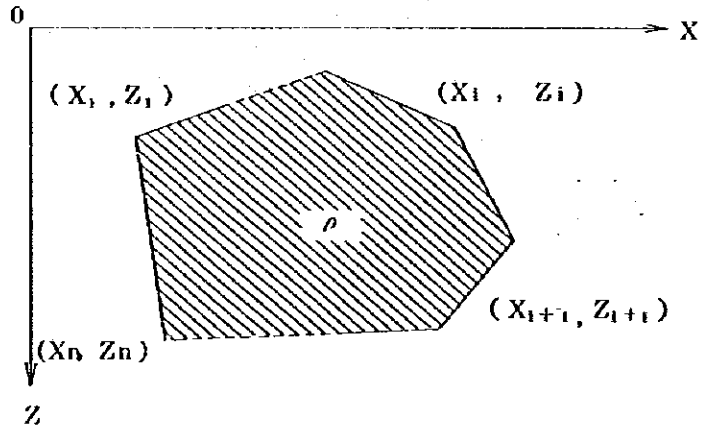

As designing initial structure models is important for modeling calculations, a multi-layer structure was initially assumed by using geological informations basing on the two-layer structure. Densities of each model were taken from Table II-3 (Distribution of Rock Densities). The initial densities of each layer were given by using following general figures:

ρ = 2.40	Quaternary, Tertiary, Upper Cretaceous, Lower Jurassic, Permo-Triassic
ρ = 2.60	Granites
ρ = 2.80	Crystalline Schists

Residual gravity values of the second order were used for all quantitative analysis involved in this survey.

2-3-6 Three-Dimensional Analysis

The residual gravity map of the second order described in "2-3-3 Trend Analysis" was studied and residual gravity values at grid points, intervals of 500 m were read. These residual gravity values at grid points were used for three-dimensional modeling calculation of a two-layer structure.

This calculation was carried out assuming an underground structure to be a two-layer structure and density difference between an upper (first) layer and a lower (second) layer to be roughly $\Delta\rho = 0.2$ g/cm^3 obtained from rock sample density measurements. To calculate gravity values of a given model, the second layer is divided into prisms with 500 m square and varying thickness of each prism by the least square method, and calculated gravity values were made to coincide with residual gravity values at every grid point.

The formulae for the calculation and the schematic diagram are as follows:

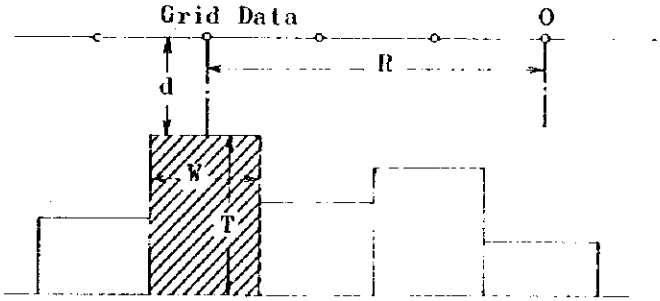

If three-dimensional prisms are placed, being their centers at each grid point as shown in the figure, a vertical component of gravity value at grid point (0) due to a prism shown by oblique lines in the figure is express in the following formula:

$$\Delta g \simeq G\rho W^2 \left\{ \frac{1}{\sqrt{R^2 + d^2}} - \frac{1}{\sqrt{R^2 + (T+d)^2}} \right\}$$

However, the following formula is used only for the prism, right under the grid point (0).

$$\Delta g_0 \simeq 2\pi G\rho \left\{ T - \sqrt{(T+d)^2 + \frac{W^2}{\pi}} + \sqrt{d^2 + \frac{W^2}{\pi}} \right\}$$

where

G : Gravitational constant
ρ : Prism density ($\Delta\rho = 0.2$)
W : Prism width = grid interval
d : Depth from the ground surface
R : Distance to the center of a prism
T : Prism height from the standard surface

The calculation was carried out iterately until the total sum of gravitational attraction from whole prisms, which is a gravity anomaly value at a grid point (0), coincides with a residual gravity value at the same point (0) by varying depth (d) of every prism.

The results were on an underground structure map where a surface of the second layer is indicated by contour lines and also geological interpretations are added.

2-3-7 Explanation of the Tables of Gravity Calculations

All correction calculations were carried out by the electronic computer model FACOM M160-AD. Computer outputs are compiled in the appendices.

(a) Earth Tide Correction and Drift Correction (Table II-1)

This table deals with gravity values at each measuring station reduced from observation values by using each correction such as earth tide, drift, instrument height and by converting to gravity standard value. On this table the following items are described from left to right.

Y M D year, month, day of observation performed
NO station number
TIME day, hour, minute

READING	observed value
INST. H	instrument height (cm)
X FACT.	observed gravity value (mgal)
ETCOR	earth tide correction (mgal)
INST. COR	instrument height correction (mgal)
+ COR	corrected value (mgal)
DRIFTCOR	drift correction (mgal)
GRVTY DIF.	difference from standard gravity value at the base station (mgal)
GRVTY VAL.	gravity value (gal)

(b) Topographical Correction (Table II-5)

This table indicates Far, Middle, Near, and adjacent topographical correction values and total values at every station. On the table the follwoings are described in the order of left to right.

STATION-NO	station number
LATITUDE (Y)	N-S distance (m)
LONGITUDE (X)	E-W distance (m)
ALTITUDE	station altitude (m)
FAR	far topographical correction value (mgal)
MIDDLE	middle topographical correction value (mgal)
NEAR	near topographical correction value (mgal)
CLOSE-1, -2	adjacent topographical correction value (mgal)
SEA	sea water correction value (mgal)
LAKE	lake water correction value (mgal)
TOTAL	total topographical correction value (mgal)

Here, density of $\rho = 2.0$ g/cm^3 was taken as a general density of the ground for calculations.

(c) Altitude Correction and Latitude Correction (Table II-6)

In this table Bouguer anomaly values are calculated and altitude correction, topographical correction, and latitude correction are also included. On the table the followings are described in the order of left to right:

STATION-NO	station number
LATITUDE (Y)	N-S distance (m)
LONGITUDE (X)	E-W distance (m)
ALTITUDE	station altitude (m)
G.V.-S.V.	gravity value corrected latitude correction (mgal)
2.00 ~ 2.80	Bouguer anomaly values calculated by using six different densities (mgal)

Chapter 3 Survey Results

The following principal charts (scale 1:50,000) were prepared, based on this gravity survey:

Pl. II-1 Locations of Gravity Stations and Their Altitudes

Pl. II-2 Bouguer Anomaly Map (Reduction density: ρ =2.5)

Pl. II-3 Residual Gravity Map in Polynomial of Second Order

Pl. II-4 Intermediate Wave-Length Bouguer Anomaly Map

Pl. II-5 Contour Line Map of Depth from Ground Surface to Basement Rocks

Pl. II-6 Profile of Underground Structure A - B

Pl. II-7 Profile of Underground Structure C - D

Pl. II-8 Interpreted Map of Underground Structure

The followings are reference charts prepared at the time of trend analysis and charts (scale 1:200,000) prepared through compilation with survey results of the previous year:

Fig. II-8 Bouguer Anomaly Map on Haute Moulouya Area

Fig. II-9 Compiled Bouguer Anomaly Map (ρ=2.5)

Fig. II-10 Regional Gravity Trend in Polynomial of Second Order

Fig. II-11 Regional Gravity Trend in Polynomial of Third Order

Fig. II-12 Residual Gravity Map in Polynomial of Second Order

Fig. II-13 Intermediate Wave-Length Bouguer Anomaly Map

Fig. II-14 Contour Line Map of Depth from Ground Surface to Basement Rocks

Fig. II-15 Profiles of Underground Structure

Fig. II-16 Interpreted Map of Underground Structure

This chapter discusses gravity distribution in the gravity charts of Pl. II-2~Pl. II-4 and Fig. II-8~Fig. II-13. --- Pl. II-5~Pl. II-8 and

Fig. II-14 ~ Fig. II-16 will be discussed in Chapter 4 in connection with geological structure.

3-1 Bouguer Anomaly Map

3-1-1 General Features

Pl. II-2 (Fig. II-9) is a Bouguer anomaly map using ρ=2.5 as a reduction density. Bouguer anomaly values in this surveyed area were approximately between -88 mgal and -113 mgal, thus indicating great negative anomalies. Since this surveyed area is in a highland such as Moyen Atlas and Haut Atlas mountains, these negative anomalies seem to be due to the so-called isostasy, theory that a Mohorovicic boundary surface is deeper under a large mass of high mountains.

As can be seen from the appended Fig. II-8 showing the general gravity distribution and topography around the surveyed area, the surveyed area is between the Moyen Atlas and Haut Atlas mountains of 2,000m to over 3,000m and forms a large mountainous region, as a whole. Since the gravity distribution in Fig. II-8 is reducted by a correction density of ρ=2.67, the minimum Bouguer anomaly value is expressed by a much smaller figure of under -140 mgal. Bouguer anomaly values ranging from -75 mgal to -140 mgal are shown but in the Mediterranean coast to the north and in the Atlantic coast to the northwest, the average of Bouguer anomaly values is about 0 mgal.

The correlation between elevation and Bouguer anomaly verifies the existence of isostasy. Similar examples have been observed in the Rocky mountains in North America, the Andes mountains in South America, and the Tibet plateau in Asia.

The gravity distribution in Pl. II-2 (Fig. II-9)(Bouguer Anomaly Map) is characterized by the fact that the surveyed area is represented by bowed isogal lines that are curved to the north, as a whole.

Gravity values slowly increase toward the north from the low-gravity zone near Zayda at the south end of the surveyed area and the gravity gradient gradually increases in the northern direction. This tendency is clearer in Fig. II-9 (Compiled Bouguer Anomaly Map). Gravity values increase, changing the gravity gradient toward the north and the east in concentric circles with the low-gravity anomaly south of Bou Mia as the center, and culminate in the prominent high-gravity anomalies in the northeastern and northwestern parts of the surveyed area.

Perhaps, this feature reflects not only the basement structure in the surveyed area but also the large basement structure around the surveyed area or deep underground. On the northwest side of the surveyed area, the Moyen Atlas mountains lie in the NE-SW direction with a basement of crystalline schists which are high-density rocks while, on the east side, there are outcrops of crystalline schists over a large area. Granites, which are the main basement rocks in the surveyed area, penetrate these crystalline schists and the gravity trend due to the density difference between both basements seems to dominate the tendency of gravity distribution.

3-1-2 Local Features

There are very few closed gravity anomalies in the Bouguer anomaly map and the gravity anomalies in it are expressed by the directions, denseness and curves of isogal lines. These gravity anomalies are often reproduced as closed anomalies or clearer anomalies by eliminating the above-mentioned gravity trend. So, only remarkable gravity anomalies are discussed here while leaving the details of local gravity anomalies for later discussion in "3-3 Residual Gravity Map in Polynomial of the Second Order".

(a) A high-gravity anomaly accompanied by dense isogal lines in the NE-SW direction is found at the northwest end of the surveyed area. It has a steep gravity gradient of about 5 mgal/km at maximum and suggests the existence of a fault structure in the NE-SW direction.

(b) A rectangular high-gravity anomaly of about 50 km² is in the eastern part of the surveyed area. A high-density rock mass is presumed to underlie in correspondence to this high-gravity anomaly.

(c) In the district from the vicinity of Zayda to the northeast of Zayd and indicated by gravity values of -112.5 mgal ~ - 107.5 mgal, the gravity gradient is, indeed, gentle, ranging from 0.3 ~ 0.5 mgal/km. Further, isogal lines in this district have many curves. These facts seem to suggest a density variety at a shallow underground level and or the undulation of the basement.

3-2 Regional Gravity Trend Maps

As mentioned already, this survey involved the conduct of trend analysis as a means of eliminating the regional gravity trend appearing in the Bouguer anomaly map and quantitative analysis using the residual gravity map in polynomial of the second order. However, this gravity trend reflects not only factors outside the surveyed area but also the basement structure in the surveyed area. Thus, if trend analysis is carried out without consideration of these conditions, there is the fear that it may also eliminate gravity anomalies caused by the basement structure in the surveyed area.

Under these points of view, the analysis was carried out by compiling gravity map for the surveyed area and its vicinities prior to the analysis in accordance with the results of the previous year's gravity survey and the existing geophysical data (Solaini L. 1965) and thus using

data of a wide area in an effort to increase the accuracy of analysis in the surveyed area.

A gravity trend map shows the regional gravity anomaly in a Bouguer anomaly map mathematically approximated to a curved-surface and well indicates an overall gravity trend because local anomalies are eliminated. The more advanced the polynomial order of the approximate curves is, the more the approximate curves follow the Bouguer anomaly map. So, it works toward the disappearance of a long-wave gravity anomaly in the residual gravity map. It is, therefor, necessary to select a regional gravity trend map or a residual gravity map after comparatively studying the relation between the geological structure of the surveyed area and these gravity distribution.

3-2-1 Regional Gravity Trend of the Second Order

A regional gravity trend map in polynomial of the second order is shown in the appended Fig. II-10. It shows great negative gravity anomalies of -115 mgal ~ -93 mgal due to isostasy, as mentioned already.

The regional gravity trend map of the second order is always indicated by parabola isogal lines. If the line connecting the vertices of these parabolas is considered as the axis of the regional gravity trend, there is a low-gravity anomaly axis in the NE-SW direction from the north side of Sidi Ayyad to the south of Bou Mia and the tendency of the lineament is to decrease and disappear in the southwestern direction with a nearly rectilinear gradient of about 0.3 mgal/km along this axis. Further, gravity gradient to the northern and southwestern directions clearly reflects the regional tendencies in Fig. II-8, particularly those outside the surveyed area.

The purpose of gravity trend analysis is to reproduce only the relation between the geological structure in the surveyed area and its

gravity distribution by finding and eliminating gravity trends occurring to the geological structure in the environs of the surveyed area or deep underground, as mentioned in "3-1-1".

From this point of view, it is necessary to pay attention to the crystalline schists being outside the surveyed area and believed to be major cause of the gravity trends.

The Moyen Atlas mountains whose basement is composed of crystalline schists are located to the northwest and north of the surveyed area and their southern edge is demarcated by a boundary line in the NE-SW or NEE-SWW direction. Also, crystalline schists crop out south of Sidi Ayyad, caused by faults running in the NE-SW direction. Comparison between this occurrence of crystalline schists and the gravity distribution in Fig. II-10 shows that there is clearly something in common. Namely, gravity values are high to the north of Itzar and in the vicinity of Mibladane and the directions of the isogal lines agree with the above-mentioned boundary lines of the crystalline schists.

From the above, it seems that the regional gravity trend map in polynomial of the second order reflects the relation between the crystalline schists existing outside the surveyed area and the component rocks in the surveyed area. Thus, the residual gravity map in polynomial of the second order can be considered to show the geological structure in the surveyed area.

3-2-2 Regional Gravity Trend of the Third Order

A regional gravity trend map in polynomial of the third order is shown in the appended Fig. II-11. Though gravity trends of the third order generally resemble trends in the regional gravity trend map of the second order, they show a smoewhat more complicated curved-surface.

In the regional gravity trend map of the third order, the axis of

low-gravity anomaly, which is rectilinear in the regional gravity trend map of the second order, bends and the gravity gradient along this axis changes in the district east of Zayda where the Zayda Granite Body crops out. Further, isogal lines in the vicinities of Mibladane and Bou Mia bend in directions different from the direction in which the occurrence of crystalline schists is controled, as mentioned above.

The gravity trend map in polynomial of the third order is considered to be undesirable, compared with the gravity trend map of the second order, because it shows not only gravity trends caused by factors outside the surveyed area but also the tendency to show the basement structure in the surveyed area.

3-3 Residual Gravity Map in Polynomial of the Second Order

A residual gravity map is a Bouguer anomaly map where a gravity trend is subtracted. In it, regional gravity distribution is put aside and the local gravity distribution is detected. The higher order of polynomial, the smaller gravity anomalies are emphasized.

In deciding which residual gravity map should be used for analysis, residual gravity maps of both the second order and the third order were prepared and comparatively studied. As the result, a residual gravity map in polynomial of the second order (to be referred to hereafter simply as a residual gravity map) believed quantitatively to express better the structure of the basement granites was selected and used for quantitative analysis of two and three-dimensional modeling calculations.

Pl. II-3 (Fig. II-12) is the residual gravity map. In Fig. II-12, the residual gravity map was prepared by conducting gravity trend analysis separately for this surveyed area and the area of the previous year's survey. So, only Pl. II-3 is used in the following explanation while

using Fig. II-12 merely as a reference map.

The maximum residual value and the minimum residual value in the residual gravity map are approximately +9 mgal and -3 mgal, respectively, and the difference is about 12 mgal. With the exception of the high-gravity anomalies occurred at the northwest end and in the eastern part of the surveyed area, the residual values in most of the area are approximately +1 ~ -3 mgal: thus the gravity distribution may be considered to be generally even.

It is most characteristic of the residual gravity map in comparison with the Bouguer anomaly map that, in the central part of the surveyed area, gravity values increase in the northern direction in the Bouguer anomaly map but reversely they decrease in that direction in the residual gravity map. Accodingly, a high-gravity anomaly exists in correspondence to the Zayda Granite Body outcrops on the east of Zayda while, in the north where the basement lies underground, there is transition to a low-gravity anomaly. In other words, the residual gravity map also expresses the relation between the basement and the overlayers. Thus this map underscores the effectiveness of the gravity trend analysis.

Further, the residual gravity map not only shows sporadic closed gravity anomalies which the Bouguer anomaly map fails to express but also reproduces small-scale gravity anomalies as accentuated isogal-line curves. Moreover, it shows great changes in the directivity of isogal lines and the continuity of gravity anomalies.

Details of the gravity distribution in the residual gravity map are as follows:

(a) The following three zones may be mentioned for remarkable high-gravity anomalies:

① High-gravity anomaly rising by a steep gradient in the direction to the west of Itzar at the west end of the surveyed area

② Large-scale rectangular high-gravity anomaly extracted in the eastern part of the surveyed area

③ High-gravity anomaly zone extending over a large area from Zayda to the east of Zayda at the south end of the surveyed area

(b) The high-gravity anomaly in ① is indicated with dense NE-SW isogal lines in the Bouguer anomaly map but is in the NNE-SSW direction in the residual gravity map. This direction and position in the residual gravity map agree with the southern edge of the Moyen Atlas mountains adjoining the surveyed area, thus suggesting the existence of a fault structure or a basement density boundary plane running in that direction.

(c) The high-gravity anomaly in ② is surrounded by dense short-wave isogal lines. Since crystalline schists, which are high-density rocks, crop out in the south of this high-gravity anomaly, it is possible to assume that a basement of crystalline schists exist in correspondence to this high-gravity zone.

(d) The area surrounded by approximately 0 mgal isogal line in the high-gravity anomaly zone in ③ corresponds to the granites outcrops known as the Zayda Granite Body. It is presumed from this fact that, in an area with a Granites basement, a high-gravity anomaly is caused by the exposure of the Granites or their existence at a shallow depth.

Further, an N-S or NNE-SSW low-gravity anomaly of the fault type dividing this high-gravity anomaly zone into two parts is accentuated.

(e) In the central and northern parts of the surveyed area surrounded by the high-gravity anomalies in the above three zones, there is an extensive low-gravity anomaly zone.

To the east of Itzar, a low-gravity anomaly continues in the NE-SW direction between the high-gravity anomalies in ① and ③. On the southwest side of the high-gravity anomaly in ② , another low-gravity

anomaly continues in the NW-SE direction. At the north end of the surveyed area, the two low-gravity anomalies meet to become a low-gravity anomaly with the minimum residual value of -3.4 mgal and seems to extend toward the north of the surveyed area.

(f) One of the above low-gravity anomaly zones is extracted as a basin-like low-gravity anomaly including closed gravity anomalies centered around a point about 6 km north-northwest of Zayda. It is surrounded by relatively dense isogal lines and seems to show a hollow in the basement.

(g) On the north side of the Moulouya river in the central part of the surveyed area, there are many short-wave gravity anomalies to be indicated by curves in isogal lines. These mainly continue in the N-S direction and seem to reflect the undulation of a basement existing shallowly underground.

(h) At the southwest end of the surveyed area, a high-gravity anomaly indicated by a 0 mgal isogal line exists on the northern edge of the granites outcrops known as the Bou Nia Granite Body. This high-gravity anomaly and the high-gravity anomaly near Zayda are linked by a ridge-like high-gravity anomaly continuing in the approximate E-W direction. Further, NNW-SEE directivity can be assumed from the shape of isogal lines in this vicinity.

3-4 Intermediate Wave-Length Bouguer Anomaly Map

A filtered Bouguer anomaly map is a map used to select any intermediate wave-length of gravity anomalies in a Bouguer anomaly map. An wave-length Bouguer anomaly map which was eliminated the noisy gravity anomalies near the ground surface and long wave-length gravity anomalies reflecting the structure at great ground depths was employed in this survey.

Pl. II-4 (Fig. II-13) is the intermediate wave-length Bouguer anomaly map. The gravity distribution in this map is divided into parts showing

certain directivity in the shape or arrangement of gravity anomalies and parts not showing any directivity in either shape or arrangement.

Main features of the gravity distribution in the intermediate wavelength Bouguer anomaly map are as follows:

(a) A positive anomaly zone extending over a large area was discovered in the eastern part of the surveyed area. This positive anomaly zone corresponds to the large-scale high-gravity anomaly indicated in the residual gravity map.

Generally, assuming a two-layer subterranean structure, a high-gravity anomaly (or positive anomaly) corresponds to an upheaval of the basement while a low-gravity anomaly (or negative anomaly) corresponds to a hollow. However, the basement in this general zone, unlike that in other districts, is presumed to be composed of high-density crystalline schists and it is impossible to assume a two-layer structure. It is, therefore, reasonable to consider that the 0 mgal line enclosing this positive anomaly zone represents the general boundary between two types of basement -- rather than discuss basement depths.

(b) On the southeast side of the above positive anomaly zone, there is a prominent NE-SW negative anomaly suggesting a graben-like structure with a width of about 1.5 km. On the southwest side of this positive anomaly zone, another negative anomalies continues in the NW-SE direction.

(c) A negative anomaly zone accompanied by closed anomalies continues in the NNE-SSW direction about 3 km east of Zayda. As is clear from Fig. II-13, it continues into the area of the previous year's survey, rectilinearly conneeting for aout 20 km from drilling point MR-1 to drilling point MR-3.

On the west side of this negative anomaly zone, positive anomalies occupy a larger proportion and, macroscopically, they can be regarded

as a positive anomaly zone arranged in the same direction: NNE-SSW. The existence of a fault structure in the general line of contact of these negative and positive anomaly zones can be presumed from the sharp contrast between the two.

(d) On the east of Itzar, closed positive anomalies exist sporadically in an NNE-SSW arrangement. These positive anomalies have been recognized from the residual gravity map merely as bulges in gravity anomalies. In fact, they seem to suggest upheavals of the basement.

On the west side of these positive anomalies, there is negative anomalies running in parallel to them and in the same direction.

(e) At the northwest end of the surveyed area, NWW-SEE positive and negative anomalies are in alternate arrangement along the Agarsif river.

Chapter 4 Underground Structure Estimated from Survey Results

In this chapter, gravity distribution and the surface geology are compared, then a quantitative study is made by two-dimensional cross-section analysis and three-dimensional analysis and underground structure in the surveyed area is estimated, based on the gravity survey.

The following table is a summary of ages of the important formations, rock names and occurrence areas used in the following discussions. In it, the classification of formation names and rock names is based on the geological survey conducted this year.

Geological Age		Geological Unit and Mark	Lithology	Area of Occurrence
Cenozoic	Quaternary	(Q_1, Q_2, Q_3)	terrace deposit, conglomerate, siltstone, mudstone	These formations not only cover the large eastern half of the surveyed area but also occur on a small scale along rivers in the western half.
		(β_{Qv})	basalt lava	This occurs on a small scale in the northern part of the surveyed area and northeast of Zayda.
	Tertiary	(T_1, T_2, T_3)	marl, limestone, siltstone, conglomerate, sandstone	These occur as hills mainly about Itzer in the western part of the surveyed area.
Mesozoic	Upper Cretaceous	Turonian (K_{2t})	micritic limestone, muddy siltstone, turbidite, calcareous siltstone	This occurs in the western part of the surveyed area and conformably covers the K_{2cm} shown below.
		Cenomanian (K_{2cm})	limestone, gypsum bed, calcareous siltstone, poly-colored siltstone	This occurs from the western part to the northern part of the surveyed area.
	Lower Jurassic	Lias (J_1)	limestone, siltstone, marl, sandstone, conglomerate, turbidite, dolomite	This occurs on the ground surface adjacently to the western edge of the surveyed area.
	Permo-Triassic	(β_{P-T})	basalt lava, sandstone, conglomerate	This not only occurs from the central part to the northeastern part of the surveyed area in the E-W direction but is also confirmed only on the west side of the fault at the western edge of the surveyed area.
		(P-T)	red sandstone, arkose sandstone, siltstone, mudstone	This occurs from the central part to the eastern part of the surveyed area, mainly covering the surroundings of basement Granites.
Proterozoic + Paleozoic	Paleozoic + Precambrian	(Gr)	granite	Part of the Zayda Granite Body crops out with NE-SW faults at the southeast end of the surveyed area from Zayda to Sidi Ayyad.
		(Gr-Dio)	granodiorite	This is known to intrude on a small scale on the south side of Sidi Ayyad east of the surveyed area.
		(Sch)	sericite-chlorite schist, amphibole schist, amphibolite	This not only sporadically exists in the watershed of the Sidi Ayyad river flowing east in the eastern part of the surveyed area but are also known to crop out on a large scale southeast of the area.

4-1 Correlation between Gravity Distribution and Geology

As mentioned already, the general gravity distribution in this area in Pl. II-2 (Bouguer Anomaly Map) is characterized by the fact that there are arch-like isogal lines in the northern direction from the low-gravity anomaly in the southern part of the surveyed area. This feature is caused by the strong effect of the Paleozoic Precambrian crystalline schists forming the basement of the Moyen Atlas mountains to the north of the surveyed area and those cropping out in the vicinity of Nibladane to the southeast of the surveyed area. In the density distribution of rock samples in Table II-3, the average density of crystalline schists is approximately ρ =2.8, which is considerably higher than ρ=2.6 for the Granites, the main basement rocks in this area.

Pl. II-3 (Residual Gravity Map in Polynomial of Second Order) obtained with the purpose of eliminating such effects from outside the surveyed area was considered to reflect the relation between the basement Granites and the sedimentary rocks that cover them. However, the analysis was conducted, taking into consideration the high-gravity anomalies found in the surveyed area which seemed to reflect a basement of crystalline schists. These correspond to the remarkable high-gravity anomalies at the northwest end and in the eastern part of the surveyed area.

The relation between the characteristic gravity anomalies in the residual gravity map in Pl. II-3 (Fig. II-12) and the intermediate wave-length Bouguer anomaly map in Pl. II-4 (Fig. II-13) and the geology (see geological map in Fig. II-5) is discussed below:

(a) The relation between the formations occurred in this area and the gravity distribution in the residual gravity map may be generally divided as follows:

① Remarkable high-gravity anomaly zones suggesting a basement of

crystalline schists

② A high-gravity anomaly zone shown by a gentle gradient reflecting the outcropping of the Granites or their existence at shallow depths

③ Areas other than ① and ② where residual values gradually decrease, leading to low-gravity anomalies

(b) The ① zones are shown by the high-gravity anomalies existed at the northwest end and in the eastern part of the surveyed area. The former is indicated by the dense NNE-SSW isogal lines and the fault in Fig. II-5 corresponds to it. On the west side of this fault, the basement is presumed to be of crystalline schists while, on the east side, it is presumed to be of Granites. In the eastern part of the surveyed area, crystalline schists partially crop out on the ground surface and crystalline schists are believed to underlie widely at shallow depths in correspondence to the high-gravity anomaly.

(c) As outcrops of the Granites which are the main basement rocks in the surveyed area, there are not only the Zayda Granite Body cropping out on the east of Zayda but also the outcrop of Granites known as Bou Mia Granite Body near the southwest end of the surveyed area. The high-gravity anomaly zone in ② is formed in general agreement with the occurrence of both granite bodies; thus it is presumed that, in areas without the occurrence of crystalline schists, the Granites cause high-gravity anomalies.

(d) These Granites can be divided into such lithofacies as granite (Gr), contaminated granite (Cnt-Gr) and aplitic granite (Ap-Gr). Little gravity change due to the variation of these lithofacies is apparent in the gravity maps. This is idential with the fact that there is no significant difference between the average densities of the various lithofacies in the density distribution of rock samples in Table II-3.

Though many NNE-SSW faults in the Zayda Granite Body have been confirmed through geological survey, gravity anomalies in this sector tend to be arranged in the same direction also in the intermediate wavelength Bouguer anomaly map. This seems to reflect density decrease due to such causes as the fractures accompanying the development of faults.

(e) The ③ areas which occupy the most part of the surveyed area are covered with Permo-Triassic and later sedimentary rocks. Mentioned in ascending order, Permo-Triassic P-T Red Sandstone Formation and β_{P-T} Basalt Formation, Cretaceous K_{2cm} Mudstone Formation and K_{2t} Limestone Formation, Tertiary T_1 Mudstone Formation·T_2 Marl Formation·T_3 Sandstone Formation, and Quaternary Q_1 Siltstone Formation·Q_2 Siltstone Formation·Q_3 River Sediments occur in an approximately horizontal sedimentary structure.

It is difficult to recognize gravity anomalies for specific formations from the comparison between the surface occurrence of these various formations and the gravity distribution in the residual gravity map. This is verified by the fact that there is no great contrast in the density distribution of the above-mentioned sedimentary rocks in Fig. II-3 as it concentrates at about ρ=2.40.

It should be considered, therefore, that the gravity distribution in these areas does not reflect any specific formation but shows the relation of the thickness of overlayers as a whole, namely, that merely the basement depth increases as the residual value decreases.

(f) In the results of the density measurements of rock samples, the average density of $\beta_{Q?}$ Basalt lava is the highest at ρ=2.82. In the surveyed area, there are sporadic small-scale lava flows but the gravity distribution corresponding to these does not show any high-gravity anomaly. It is considered, therefore, that $\beta_{Q?}$ Basalt lava existing

sporadically in this surveyed area is so thin that it is not reflected as a gravity anomaly.

4-2 Contour Line Map of Depth from Ground Surface to Basement Rocks

Pl. II-5 (Fig. II-14) is a contour line map of depth from ground surface to basement rocks by a two-layer structure.

This map was prepared, based on the results of the three-dimensional modeling carried out by setting the density difference of 0.2 g/cm³ between the upper and lower layers and using the value of residual gravity in polynomial of the second order. However, the surveyed area includes places with the occurrence of crystalline schists and a two-layer structure cannot be assumed for these places and their vicinities. So, the contour line map of depth from ground surface to basement rocks was prepared by making approximate curved-surface correction using the results of profile analysis by two-dimensional modeling, position of the basement rock outcrops and the results of drilling survey.

Further, according to drilling MR-3 conducted in the area of the previous year's survey, the proportion of Tertiary and Quaternary formations whose densities are smaller among the sedimentary formations covering the basement is very large (see Table II-3). So, a second analysis using 0.25 g/cm³ as the density difference between the basement Granites and the formations covering them was carried out. The results of this analysis are compiled and shown in Fig. II-14.

Here, mainly the structure relating to basement depths is described since the contour line map of depth from ground surface to basement rocks represents the underground depth of the surface of basement rocks. For the basement structure discussed from the view-point of altitudes above sea level, see "4-4 Interpreted Map of Underground Structure".

The basement structure in this area, as presumed from the contour line map of depth from ground surface to basement rocks in Pl. II-5 (Fig. II-14), is as follows:

(a) The thickness of the sedimentary formations covering the basement in the surveyed area is greatest (about 480 m) north of Itzar but is less than 200 m in about a half of the entire surveyed area.

(b) There are Granites outcrops known as Zayda Granite Body and Bou Mia Granite Body, respectively, on the east of Zayda and northwest of Bou Mia.

The basement underlies at a shallow depth of about 100 m in the E-W direction connecting the two granite bodies. This suggests that the two rock bodies are united underground.

(c) The sedimentary structure covering the basement in the surveyed area greatly differs between the eastern half and the western half of the area. In the eastern half, the sedimentation does not exceed 200 m in thickness and the thickness gradually increases in the northern direction from the Granites outcrops on the southern edge. Generally contour lines of E-W direction are accentuated.

In the western half, basement contour lines are generally in the NE-SW direction and the formation thickness increases in the northwestern direction and reflects the relation with the topography in which altitude increases in the same direction. In further details, formation thickness suddenly increases from the basement depth of about 200 m and, in most part, the sedimentation is relatively thick, ranging from about 200 m to more than 400 m.

(d) On the south side of Zayda, the results of the second analysis conducted in the area of the previous year's survey (see Fig. II-14) show that the basement depth is up to 200 m in the large part and the basement dips sharply in the southwestern direction to reach a depth of more than

700 m south of Bou Mia.

4-3 Profiles of Underground Structure

Profiles of underground structure were prepared by carrying out two-dimensional modeling calculations using residual gravity values on two E-W sections: A - B (Pl. II-6) and C - D (Pl. II-7), as indicated in each gravity map.

Each plate shows profiles in the following order from top to bottom:

(a) Bouguer Anomaly: ρ =2.5

(b) Residual Gravity in Polynomial of Second Order

Here, the results of two-dimensional modeling calculations at intervals of 500 m are indicated as 'Estimated Gravity Values'.

(c) Intermediate Wave-Length Bouguer Anomaly

(d) Radon Etch Anomaly

The results of radon etch survey (unit: Tracks/square millimeter· 30 days; to be indicated hereafter as T/mm²) and the results of gravity analysis are shown comparatively.

(e) Underground Structure

The results of two-dimensional modeling calculations carried out, using mainly a two-layer structure and, if necessary, adding a third layer, are indicated by the boundary lines between each layer and by their densities.

Formations corresponded to each density layer are set as follows:

I	ρ =2.4	Quaternary, Tertiary, Cretaceous and Permo-Triassic formations
II	ρ =2.6	Granites
III	ρ =2.8	Crystalline schists

(f) Geological Structure

The geological structure was presumed mainly from the basement structure obtained from the above-mentioned modeling calculations and taking horizontal interpretations and geological information into consideration. Further, the basement depression that will be mentioned in "4-4 Interpreted Map of Underground Structure" is also used here; it is described under the definition of fault-like step structure.

Each profile in Pl. II-6 and Pl. II-7 is on a scale of 1/50,000 in the horizontal direction but the scale in the vertical direction used for (e) Underground Structure and (f) Geological Structure is 1/10,000.

The underground structure in each profile is presumed as follows:

4-3-1 A-B Profile

Pl. II-6 (Fig. II-15-a) is the A-B profile. This profile is set in the E-W direction passing through three drill holes: MR-1, MR-2 and MR-4 and is aimed, primarily, to see the basement structure as a whole, taking advantage of known basement depths.

The main surface geological occurrence in this profile does not show any outcrop of basement rocks and the lower P-T Red Sandstone Formation crops out in the central part of the profile. On the top of this formation, β_{P-T} Basalt Formation, Q_2 Siltstone Formation and Q_3 River Sediments are accumulated in ascending order in the eastern half of the profile. In the western half of the profile, topographical altitude gradually increases in the western direction and β_{P-T} Basalt Formation, K_{2cm} Mudstone Formation, K_{2l} Limestone Formation, T_1 Mudstone Formation, T_2 Marl Formation, T_3 Sandstone Formation, Q_1 Siltstone Formation and Q_3 River Sediments are accumulated in ascending order in the western direction, reflecting topographical altitudes. At the west end of the profile, a fault clearly dividing the sedimentary structure is developed and each

gravity profile shows sharp gravity change in correspondence to this. Further, the basement at the three drill holes: MR-1, MR-2 and MR-4 is invariably composed of the Granites and its reported depth is 144.80 m, 264.90 m and 372.00 m, respectively.

In the residual gravity profile, there is an impressive contrast between the gentle low-gravity anomaly zone continuing from the center of the profile to the western part and the prominent high-gravity anomaly zones located at the west end of the profile and in the eastern part. Particularly, the high-gravity anomaly in the eastern part is on a large scale with a width of 10 km and a residual value of about 5 mgal at its apex.

The following underground structure can be presumed from the geological structure profile based on the results of analysis:

(a) Nearly vertical fault-like step structures F-① and F-④ are presumed to exist at the east and west ends of the profile and these structures are believed to form boundary planes between basement Granites and crystalline schists.

(b) Crystalline schists are considered to underlie for about 10 km as the basement in the vicinity of the Sidi Ayyad river and were analyzed that they underlie at a shallow depth of less than 150 m. The intermediate wave-length Bouguer anomaly profile shows a positive anomaly corresponding to them.

(c) Basement depth from the ground surface is minimal (several 10 m) near Station No. 887 in the eastern part of the profile and maximal (more than 400 m) near Station No. 250 in the western part of the profile. But in terms of basement elevation above sea level, these are within the limit of about 1,250 m to 1,350 m and can be regarded as presenting a generally horizontal basement structure. It is considered that the

structure of sedimentary rocks is also approximately horizontal in harmony with the basement structure.

(d) Hollows considered to be channels on basement Granites have been found to exist underground near Stations Nos. 587 and 140 in the central part of the profile. The maximum depth of these is presumed to be about 200 m from the ground surface at both places.

4-3-2 C-D Profile

Pl. II-7 (Fig. II-15-b) is the C-D profile. The C-D profile is 4 km away to the south side of the A-B profile and parallels it. It is aimed, primarily, to detect hollows on the shallow-lying basement in the eastern half and clarify the undulation of the basement at deep underground in the western half.

In this profile, the surface geological occurrence consists, mainly, of the sporadic outcrops of basement Granites and the thin P-T Red Sandstone and Q_2 Siltstone Formations covering them in the eastern half of the profile. In the western half of the profile, a sedimentary structure exists which is almost the same as in the A-B profile. The whole profile is characterized by the fact that, with the exception of the west side of the fault existing at the west end of the profile, no β_{P-T} Basalt Formation occurs on the ground surface.

In the residual gravity profile, relatively unchanging residual values ranging from -3 mgal to +2 mgal are shown except for the high-gravity anomaly at the west end of the profile. However, the whole profile presents gravitational changes with many short-wave bends. In the intermediate wave-length Bouguer anomaly profile, this is accentuated and there are evident gravity anomalies.

The following underground structure is presumed from the geological structure profile resulting from analysis:

(a) There are many fault-like step structures reflecting undulation or depression of the basement. F-① is a large fault restricting occurrence of basement Granites and crystalline schists, F-② and F-③ show vertical depression of Granites, and F-④ and F-⑤ suggest the existence of a graben-like structure between the two.

(b) In this profile, the basement is mostly composed of Granites but crystalline schists seem to occur partially on the west side of the fault-like step structure and near Station No. 944.

(c) Basement and sedimentary structures greatly differ between the eastern half and the western half of the profile. In the eastern half, the basement underlies at a shallow depth or crops out while, in the western half, the basement underlies at a depth of more than 400 m, at maximum, and thick sedimentary rocks cover it. As for basement altitudes, the average elevation is about 1,400 m in the eastern half but 1,100 m to 1,300 m in the western half, the difference being about 200 m.

Compared with the A-B profile, only the eastern half of the C-D profile turns upward.

(d) The whole profile shows a basement surface with many undulations. Particularly, east of Aït Ghiat there are sporadic hollows with depths of 20~80 m believed to be channels on basement rocks.

Radon etch anomalies tend to appear in correspondence to these hollows. It must be especially noted that radon etch anomalies of more than 400 T/mm² have been measured between Stations Nos. 644 and 164.

4-4 Interpreted Map of Underground Structure

Pl. II-8 (Fig. II-16) is the interpreted map of underground structure. In this map, the results of comprehensive analysis are indicated by the following method and numbered at need.

(a) Contour Lines of Surface of Basement Rocks

These lines are in terms of altitudes above sea level into which contour lines of depth from the ground surface to the basement rocks in Pl. II-5 were converted, using mainly station elevations, and express elevations on the surface of basement rocks.

(b) Fault-like Step Structures

These represent continuously detected steep-gradient depressions in the basement and they have been concluded that the local structures are fault-like.

(c) Channel Structures on Granites

A channel structure has been presumed by tracing continuous hollows on the basement and indicating their positions and directions.

(d) Basin Structures

These represent large-scale hollows on the basement forming particularly thick sedimentary structures.

(e) Radon Etch Anomalies

Zones with over 200 (T/mm^2·30 days) are shown by rounding 212.3 (T/mm^2·30 days) considered from the results of radon etch survey to be an anomaly.

The details of the interpreted map of underground structure are discussed below by referring to the above.

4-4-1 Presumed Basement Structure

The interpreted map of underground structure in Pl. II-8 (Fig. II-16) closely resembles the contour line map of depth from ground surface to basement rocks in Pl. II-5 (Fig. II-14) but is somewhat different, reflecting the topography in which altitudes increase in the western or northwestern direction.

In the contour line map of depth from ground surface to basement

rocks, the direction in which contour lines are arranged in the western part of the surveyed area strongly tends to be NE-SW but in the interpreted map of underground structure, this directivity is weak and in the surveyed area as a whole, the direction is E-W.

In the E-W direction connecting the Bou Mia Granite Body and the Zayda Granite Body there is a large saddle-like structure (area above 1,400~1,450 m in Fig. II-16) that continues almost horizontally. With this saddle-like structure as the apex, basement altitudes decrease on the north and south sides in the northern and southern directions, respectively. The maximum difference is about 400 m in the area of this year's survey and more than 800 m in the area of the previous year's survey.

The following features stem from this large E-W basement structure at many places:

(a) In the light of the results of geological survey, NNE-SSW or NE-SW faults are verified in the surveyed area and its vicinities (see Fig. II-5). It is presumed from the results of study of these known fault structures and gravity anomalies that there are fault-like step structures F-① ~ F-⑤ extending in the same directions.

The fault-like step structure F-① extending in the NNE-SSW direction west of Itzar generally corresponds to a fault verified on the ground surface. This is considered to be a large fault representing the vertical boundary between basement Granites and crystalline schists.

The presumed fault-like step structure F-② to the northwest of Zayda seems to continuously represent the steep dip where a large fault zone extending farther in the N-S direction or basement Granites sinks to the west side in the vicinity of this structure.

The fault-like step structure F-③ continuing in the NNE-SSW direction to the northeast of Zayda suggests fault structures accompanied

by fracture zones. From Pl. II-4 (Fig. II-13) (Intermediate Wave-Length Bouguer Anomaly Map), the structure is likely to continue farther in the northern and southern directions.

The fault-like step structures F-④ and F-⑤ running parallel in the NE-SW direction in the vicinity of the Sidi Ayyad river suggest the existence of a graben-like structure lain between these two structures. F-④ is presumed to constitute a boundary between basement Granites and crystalline schists.

(b) Many ridge-like basement structures where closed lines or bulges of contour lines showing basement depth continue have been found. Chief among them are the ridge-like structure continuing for more than 10 km in the NNE-SSW direction on the east side of Itzar, the NNE-SSW ridge-like structure adjoining the west side of the fault-like step structure F-③ northeast of Zayda and the ridge-like structure extending in the N-S direction through the basement bulge (believed to be composed mostly of basement crystalline schists) in the vicinity of the upper reaches of the Sidi Ayyad river.

These structures not only seem to control the directivity of channel structures to be described later but are also considered to be important in studying the possibility of existence of mineral deposits.

(c) A basin structure in a basement of more than 30 km² is likely to exist east of Itzar. It abruptly sinks with a depression of about 200 m on three sides: east, south and west and opens on the north side. In the area of the previous year's survey also, a large basin structure is estimated on the south of Bou Mia.

It is considered that these basin structures are filled with Permo-Triassic and later formations accumulated to a great thickness.

4-4-2 Presumed Channel Structures

As mentioned already, the basement structure in this area is composed, mainly, of the E-W saddle-like structure linking the Bou Mia and Zayda Granite Bodies and its altitude decreases in the northern direction as NE-SW or N-S fault structures and ridge-like structures are interrupted from it. This present basement structure seems to retain the original paleotopography of the Triassic and earlier periods more or less intact since the sedimentary structure covering the basement in this area is generally horizontal. However, the basement structure, no doubt, underwent some change due to later upheaval, subsidence or fault activity.

So, continuous hollows believed to be channels on the basement and low-gravity anomalies in the gravity maps have been continuously traced and indicated in the interpreted map of underground structure by their positions and directions as present channel structures on Granites.

The distribution of main channel structures can be generally divided into the following five categories:

① Several channel structures starting in the vicinity of the outcrop of the Zayda Granite Body on the east of the fault-like step structure F-③. They meet at 1.5 km east of drilling point MR-1 and proceed north.

② Channel structures running in the northern direction between the fault-like step structures F-② and F-③ with meandering and stagnation.

③ Channel structures concentrated in the basin structure east of Itzar. The main channel structures run in the northern direction from the apex of the saddle-like structure located west-southwest of Zayda and attains its greatest depth in the vicinity of the middle reaches of the Bou La'joul river.

④ Channel structure considered to exist in the graben-like structure lain between two fault-like step structures at the east end of the